




12-2016

## **Preliminary Investigation for the Development of Surrogate Debris from Nuclear Detonations in Marine-Urban Environments**

Adam G. Seybert

*University of Tennessee, Knoxville, aseybert@vols.utk.edu*

Follow this and additional works at: [https://trace.tennessee.edu/utk\\_gradthes](https://trace.tennessee.edu/utk_gradthes)

 Part of the [Nuclear Engineering Commons](#), [Other Applied Mathematics Commons](#), and the [Other Chemical Engineering Commons](#)

---

### **Recommended Citation**

Seybert, Adam G., "Preliminary Investigation for the Development of Surrogate Debris from Nuclear Detonations in Marine-Urban Environments. " Master's Thesis, University of Tennessee, 2016.  
[https://trace.tennessee.edu/utk\\_gradthes/4272](https://trace.tennessee.edu/utk_gradthes/4272)

This Thesis is brought to you for free and open access by the Graduate School at TRACE: Tennessee Research and Creative Exchange. It has been accepted for inclusion in Masters Theses by an authorized administrator of TRACE: Tennessee Research and Creative Exchange. For more information, please contact [trace@utk.edu](mailto:trace@utk.edu).

To the Graduate Council:

I am submitting herewith a thesis written by Adam G. Seybert entitled "Preliminary Investigation for the Development of Surrogate Debris from Nuclear Detonations in Marine-Urban Environments." I have examined the final electronic copy of this thesis for form and content and recommend that it be accepted in partial fulfillment of the requirements for the degree of Master of Science, with a major in Nuclear Engineering.

John D. Auxier II, Major Professor

We have read this thesis and recommend its acceptance:

Howard L. Hall, Joseph Stainback IV

Accepted for the Council:

Carolyn R. Hodges

Vice Provost and Dean of the Graduate School

(Original signatures are on file with official student records.)

**Preliminary Investigation for the  
Development of Surrogate Debris from  
Nuclear Detonations in Marine-Urban  
Environments**

A Thesis Presented for the  
Master of Science  
Degree  
The University of Tennessee, Knoxville

Adam G. Seybert  
December 2016

Copyright © 2016 by A. G. Seybert  
All rights reserved.

## **ACKNOWLEDGEMENTS**

First and most importantly, I would like to thank my wife Jodi for all of the love and support she has provided over the last ten years. Seven moves, two deployments, and two kids later, you continue to be the love of my life. I would also like to thank my research advisors for the mentorship over the last few years. I would like to thank personally Dr. John Auxier II for continually seeking out new opportunities for me to grow professionally and Dr. Howard Hall for finding the resources for me to participate in them. None of this would have been possible without the many conferences and trips you both supported. I would also like to thank Dr. Joseph Stainback IV for the advice and mentorship and always demonstrating the attributes of a true professional. I would next like to thank my fellow research-group students. Mike, Boone, Andy, Matt, and Saul, thank you for never giving up on me but also never letting me down. This work could not have been completed without the foundational works of Major Josh Molgaard and Andy Giminaro. Lastly, I would also like to thank Rob Beimler from the United States Army Nuclear and Countering Weapons of Mass Destruction Agency (USANCA) for the continued career advice and support over the last several years.

***“If I have seen further, it is by standing on the shoulders of Giants”***

**~Isaac Newton**

## **ABSTRACT**

No nuclear weapon has ever been detonated in a United States city. However, this also means the nuclear forensic community has no actual debris from which to develop analytical methods for source attribution, making the development of surrogate nuclear debris a vital undertaking. Moreover, the development of marine-urban debris presents an unusual challenge because unlike soil and urban structures, which remain compositionally consistent, the elemental composition of harbor and port waters fluctuates considerably due to natural phenomenon and human activity. Additionally, marine vessel composition and cargo can vary dramatically. While early US nuclear tests were carried out in shallow-water coastal areas, they did not represent the marine-urban environments of large cities and any residual debris will be ill suited for the development of modern forensic techniques. Given these technical complexities, it is critical to understand the environmental variations in order to develop realistic surrogate nuclear marine-urban debris. This project seeks to build a robust model for the New York/New Jersey harbor, the Port of Houston, and the Long Beach/Los Angeles harbor that statistically define the elemental composition of vaporized debris for follow-on neutron-activation and debris formation analysis. Analysis of these neutron and fractionation effects will support the development of unique surrogate debris samples that mimic the elemental content of actual nuclear debris from a marine-urban detonation. These samples can then be utilized for the development of the analytical methods for post-detonation analysis and attribution.

# TABLE OF CONTENTS

Chapter One Introduction and Background .....	1
The Marine-Urban Nuclear Risk: Threats, Vulnerability, and Consequences ....	1
Forensic Need for Post-Detonation Surrogate Material.....	3
Chapter Two Literature Review.....	6
Previous Methodologies for the Development of Surrogate and Synthetic Environmental Materials .....	6
Idaho National Lab, Sol-Gel.....	6
UT Radiochemistry Center of Excellence, Surrogate Trinitite .....	7
UT RCoE, Urban Surrogate Debris.....	7
Previous Maritime Nuclear Weapons Detonations and Characteristics.....	8
Operation Crossroads.....	8
Operation Hurricane (UK) .....	9
Operation Hardtack.....	9
Marine Debris Research.....	11
Chapter Three Elemental Characterization of Marine-Urban Layers .....	12
Layer Mass Fraction Estimation.....	12
Vessel Layer Volume .....	15
Soil Layer Volume.....	15
Infrastructure Layer Volume .....	16
Marine Layer Volume.....	16
Layer Void Fractions and Density.....	16
Weapon Elemental Contributions .....	17
Calculating Layer Mass Fraction.....	18
Elemental Characterization of Marine-Urban Layers .....	18
Marine Water and Sedimentation Layer .....	18
Marine Vessels and Vehicles .....	21
Soils and Infrastructure .....	23

Model Variable Inputs.....	24
Chapter Four Results and Discussion .....	25
Calculated Layer Mass Fraction.....	25
Elemental Weight Percent for Marine Urban Debris .....	25
Oxide Powder Weight Percent for MUD Formulation.....	31
Model and Variable Sensitivity Analysis .....	31
Ferrosilicon Production Challenges .....	34
Chapter Five Conclusions and Recommendations .....	35
Conclusions.....	35
Future Work .....	35
Neutron Activation .....	35
Environmental Fractionation .....	36
Works Cited.....	38
Appendix .....	42
APPENDIX A: STATA ANOVA Results.....	43
APPENDIX B: STATA Regression Results.....	48
Vita.....	56



## LIST OF TABLES

Table 1.1 Shipping and Population Data for the Top Five US Ports.....	2
Table 2.1 Operation Hardtack Relevant Detonations .....	10
Table 3.1 Ionic Composition of Sea Water .....	19
Table 3.2 Elemental Concentrations (ppm) for Sediment Metals .....	20
Table 3.3 Weight Percent for Vessel and Container Steel .....	22
Table 3.4 Elemental Weight Percent for Concrete (Portland) .....	23
Table 3.5 Variable Distributions for the Port of Interest.....	24
Table 4.1 Layer Mass Fraction for the Three Ports of Interest.....	25
Table 4.2 Full Elemental Mass Fraction and Standard Deviation .....	26
Table 4.3 Oxide Powder Mass Fraction for each Location .....	31
Table 4.4 Linear Model Coefficients for Top Ten Elements.....	33
Table 5.1 Refractory and Volatile Elements for Marine-Urban-Debris .....	36

## LIST OF FIGURES

Figure 3.1 Handy-size Shipping Vessel (60-Meter Scale) .....	13
Figure 3.2 Common Vessel Classes and Dimension .....	14
Figure 3.3 2D Schematic of Fireball Environment and Layers .....	15
Figure 3.4 Distribution of US Commerce by Commodity .....	22
Figure 4.1 Elemental Composition of Predicted MUD for the Port of NY/NJ .....	27
Figure 4.2 Elemental Composition of Predicted MUD for the Houston Harbor .	28
Figure 4.3 Elemental Composition of Predicted MUD for the Port of LA/LB .....	28
Figure 4.4 Mass Fraction for Top Nine Elements by Location .....	29
Figure 4.5 Mass Fraction for Salts by Location .....	30
Figure 4.6 Results of Melts/Ingots with Varying Fractions of Iron .....	34

## **CHAPTER ONE INTRODUCTION AND BACKGROUND**

### **The Marine-Urban Nuclear Risk: Threats, Vulnerability, and Consequences**

Throughout the last decade, the threat of a nuclear terror attack on a major US city has been the subject of countless agency, multiagency, and industry reports and investigations. In response to the threats, vulnerabilities, and consequences outlined therein, the US Department of Homeland Security (DHS) established a pilot program (Securing the Cities) to enhance the capabilities of local, state, and federal law enforcement to detect and interdict radiological and nuclear materials in the New York City/Jersey City/Newark region. DHS expanded this program in 2012 to include the Los Angeles/Long Beach region. This program was expanded in 2014 to include the National Capital Region and then again in 2015, establishing Houston and Chicago as participating locations [1]. While these programs address preventing nuclear attacks in the whole of the urban area, this work specifically focuses on a subset of the urban environment: urban port and harbor infrastructure.

A 2005 Congressional Research Service (CRS) Report specifically addresses the threats, vulnerabilities, and consequences of a nuclear attack on US seaports. According to the report, and others like it, US ports are a key interest to terrorist groups and present a credible threat [2][3]. At the center of US-port-vulnerability is the vastness of the material that these ports process. In 2013, nearly 28,700 tanker-ships, 17,500 containerships, and 21,000 dry-bulk and general cargo-ships arrived through US ports [4][5]. Of this traffic, the US Customs and Border Protection (CBP) only inspects about 6% [2]. Additionally, the port waterways provide high-speed avenues for smaller recreational vessels that could be used for an attack [3].

Further complicating matters, nearly all of the major US ports are located in close proximity to major urban areas. While a detailed analysis of the damage

from a port-focused nuclear attack is situationally dependent, the CRS report suggests that a 10-20 kiloton nuclear detonation in a major urban port would result in an estimated 50,000 to 1 million casualties and \$50-500 billion in economic damages [2]. Table 1.1 shows the shipping statistics for the top five largest US port complexes, in 2013, along with the population dynamics of the closest major urban areas.

**Table 1.1 Shipping and Population Data for the Top Five US Ports**

Ports	Shipping Data (2013) [4] [5]			Population Data (2010)		
	Total tons (Millions) <sup>a</sup>	Vessel Calls <sup>b</sup>	Vessel Type <sup>c</sup>	Population Center	Density (per sq mi)	Distance to City Hall (mi)
South Louisiana, LA, Port of	239	4,098	Container	New Orleans, LA	4,370	30
Houston, TX	229	8,321	Tanker	Houston, TX	4,110	23
Long Beach/Los Angeles, CA	142	3,887	Container	Los Angeles, CA	12,114	20
New York, NY and NJ	123	5,508	Container	New York, NY	31,251	<15
Beaumont, TX	94	7,462	Tanker	Beaumont, TX	1,711	<1

<sup>a</sup> Tonnage totals include both domestic and foreign waterborne trade.

<sup>b</sup> Privately-owned, oceangoing merchant vessels over 1,000 gross tons

<sup>c</sup> Dominant type of vessels in port

From Table 1.1, it is apparent that for all but the Port of Southern Louisiana, the distance from the port to the city center is less than 25 miles. We also see that except for Beaumont, TX, each city has an average population density of over 4,000 people per square mile. With the volume of shipping traffic in the Port of Long Beach/Los Angeles and the Port of New York/New Jersey, combined with the proximity to their highly populated city centers, these ports present the greatest risk for nuclear terrorism. This work will specifically focus on the ports of NY/NY, LB/LA, and Houston.

## **Forensic Need for Post-Detonation Surrogate Material**

The underlying principle of technical nuclear forensic science is the ability to examine a set of characteristics of nuclear material to identify unique signatures that experts attribute to specific locations, groups, or both. In the analysis, the nuclear material can be recovered either before a nuclear detonation (pre-detonation) or after (post-detonation). Potential perpetrators of interest typically include both state and non-state actors. Attribution in pre-detonation forensics allows the US government to identify the source of nuclear materials and ensure further materials have not been diverted from their intended use. With post-detonation analysis, being able to identify the source of a nuclear device (or rule-out countries as the source) allows the US government to leverage fully its military and political power, in addition to preventing further attacks[6][7]. Moreover, strong attributional tools can provide deterrence to potential hostile actors. This paper specifically focuses on analysis of nuclear material and debris following a nuclear detonation in the port/harbor region.

The debris created in the detonation of a nuclear device of any size is characteristic of both the weapon's design and the detonation environment. The characteristics of the debris include size, morphology, and elemental and isotopic composition. The elemental and nuclide composition of the debris can be categorized into four groups: residual nuclear fuel and device material, bulk environmental material, activation products, and fission products. In many cases, the environmental material forms the base for the debris; however, this material provides little use for attribution. Rather, the residual weapon material and fission products entrained in this bulk material provide the signatures necessary for attribution.

Nevertheless, attribution in nuclear post-detonation environments is not a trivial task. In a pre-detonation scenario, the nuclear material remains intact and in a form that is generally representative of its source. For post-detonation debris, the nuclear detonation exerts complex physical processes on the material including

intense neutron flux, extreme heat, and pressure effects. Moreover, after the detonation has vaporized the original nuclear material, complex debris formation processes and environmental transport will shape the unique nature of the debris produced. These processes can result in debris with many different combinations of residual weapon material, fission products (FP), and activation products entrained in bulk environmental material. Following these complex processes, debris collectors must find suitable debris, collect it safely, and transport it for in-depth analysis. In addition to managing resources with emergency management responders, this material must be collected while avoiding the hazards present in post-nuclear detonation environment. Once the debris arrives in the lab, forensic scientists must then chemically process this material for detailed non-destructive and destructive analysis. This processing and analysis can be incredible complex and must be conducted with care to ensure that the results of the analysis are judicially admissible.

Since the last US nuclear detonation occurred in 1992, there is a scarcity of actual debris material available to validate analytical methods, establish process standards, and train the next generation of nuclear forensic analysts. Moreover, the actual debris available has undergone significant nuclear decay and is not representative of the debris that a marine-urban detonation would produce. By developing representative surrogate debris, the nuclear forensic community can use this material to develop the analytical methods necessary for debris characterization and attribution from a marine-urban nuclear detonation.

In developing these materials, it is important to note that they need not be exact matches for nuclear debris. Because of the complex processes noted above, each debris sample from the same detonation may be markedly different in composition. Rather, as surrogates, these materials must have similar form and function to actual debris for the analytical methods to be validated. For surrogates used to validate radiation detection methodologies, these materials must have radionuclide compositions that accurately match predicted debris to within reason; however, the physical form of the surrogate may be less important. For

analysis with tools such as inductively coupled plasma – mass spectrometry (ICP-MS) and thermal ionization – mass spectrometry (TIMS), which require complete dissolution of the debris, the surrogates must have a chemical structure and morphology that is representative of predicted debris. Similarly, surrogate debris must also have surface that is chemically similar to actual debris for methods using secondary ionization mass spectrometry (SIMS). Isotopic ratios may be of little use if only validating the dissolution processes. This work specifically focuses on developing surrogates of morphologically complex debris to develop further the analytical dissolution techniques.

## CHAPTER TWO LITERATURE REVIEW

### **Previous Methodologies for the Development of Surrogate and Synthetic Environmental Materials**

The analysis of glasslike materials to infer knowledge of its formation is not a new field. Such analysis has been used in many fields including history, geology, industrial engineering, and chemical engineering, in addition to nuclear engineering. Additionally, methodologies have been developed for vitrifying powder samples for laser-based analysis [8]. Because the analysis and of vitrified materials spans many fields, there are also many different methodologies for producing synthetic/surrogate glasses to refine analytical methods. Researchers have previously used two primary methods to produce debris surrogates useful for nuclear forensic analysis. These include thermal “baking” and the sol-gel process.

#### ***Idaho National Lab, Sol-Gel***

In the solution-gel (sol-gel) process, a silicate-based sol is prepared and chemically treated to produce either a glassy or a ceramic material. Kevin Carney, Martha Finck, *et. al* have utilized the sol-gel process to produce surrogate debris for training and measurement exercises at Idaho National Laboratory (INL) [9]. For their debris, they utilized tetraethyl orthosilicate for the precursor to form the bulk matrix representative of the environmental conditions at a detonation site. The tetraethyl orthosilicate is doped with 93% HEU to represent any residual fuel material in debris. Additionally, these samples were irradiated with a thermal neutron flux of  $3 \times 10^{12} n \text{ cm}^{-2} \text{ s}^{-1}$  for 15 minutes to produce a surrogate with representative fission products.

This process is relatively cheap and requires low temperatures for glass formation. Moreover, this process has an established record, dating back to the mid-1800's, for the production of SiO<sub>2</sub> based glasses [10]. The sol-gel process also has some limited ability for doping the initial solution with organics and rare-earth



elements. While this process can produce debris that has a homogenous distribution of dopants, the production process involves extensive “wet chemistry” and the chemical form of the debris is limited mostly by the initial solution composition.

### ***UT Radiochemistry Center of Excellence, Surrogate Trinitite***

Previous efforts at the University of Tennessee’s Radiochemistry Center of Excellence (UT RCoE) to model debris production from both the Trinity test and potential urban detonation scenarios have relied on “baking” elemental “recipes” in an induction furnace. The general methodology starts by first characterizing the elemental composition of the detonation environment, then developing a mix of oxide powders that replicate the environment’s elemental mass fractions. This powder mix is then placed in a graphite crucible and melted at approximately 1400-1600°C for 20-60 minutes and then rapidly cooled in a sand bed [11].

Initial RCoE work started with a mix of oxide powders representative of standard trinitite formulation (STF). Samples were prepared by hand grinding this mix and then firing the samples in a Carbolite 18/4 High Temperature Furnace (HTF) for various durations and at various temperatures. By analyzing the surrogate trinitite, along with actual trinitite, using P-XRD, SEM, and EDS, Molgaard *et al.* was able to demonstrate that the surrogate material was physically, chemically, and morphologically accurate [12].

### ***UT RCoE, Urban Surrogate Debris***

While the analysis for the Trinity site relied on mapping the soil composition, the urban characterization method utilized a three component modeling approach [13]. The basic layers include an infrastructure layer, a vehicular layer, and a soil layer. By examining these layers for both Houston and New York, Giminaro developed unique recipes representative of these two cities.

## **Previous Maritime Nuclear Weapons Detonations and Characteristics**

With the exception of the attacks on Hiroshima and Nagasaki (which were air-bursts), no nuclear detonations have occurred in environments with both urban and marine layers; however, the results from previous weapon testing, both surface and underwater bursts, serve as the natural starting points for examining more complex detonation scenarios. First we will examine the major tests used to develop the body of debris formation knowledge.

### ***Operation Crossroads***

Operation Crossroads was the first set of tests in the Marshall Islands used to determine the viability of nuclear weapon use in naval warfare [Bombs at Bikini]. This test series consisted of two device detonations, the Able-shot and the Baker-shot. The Able-shot was a 23-kt airdrop detonation (~160m height of burst), while the Baker-shot was also a 23-kt underwater burst. Following these detonations, sensors were collected and the results analyzed to determine the effects.

We will focus specifically on some of the debris related results from the Baker test [14][15]. In addition to pressures measured in excess of 10,000 pounds per square inch near the detonation site, many fragments from the ships and lagoon bottom produced “bright tracks” and landed more than a mile from the site. Based post detonation photography, the Baker shot is estimated to have vaporized several million tons of water (best estimate is 2 million tons).

Analysis of water samples following the tests and activation foils on target ships indicate that most of the neutrons were absorbed in the water with extensive neutron absorption by hydrogen, chlorine, and other seawater elements. Notably, the high sodium ion content of the seawater resulted in the considerable production of Na-24 and Cl-38. Some of this activated radioactive material drifted in the cloud; however, most remained in the lagoon area. Collected debris included mostly small solid particles and slurries of sea-salt crystals.

### ***Operation Hurricane (UK)***

The notion of ports being a vulnerable target for nuclear attack predates the modern era. Concerned about the vulnerability of their ports, bays, and harbors, the British conducted their first nuclear weapons test in 1952 to assess these vulnerabilities. The device was loaded in the center of the H.M.S Plym, a 1,450-ton frigate. On the morning of October 3<sup>rd</sup> the British detonated their plutonium-based device off the shores of the Monte Bello Islands. Similar to the US tests, the British reported thousands of tons of water, mud, and rock pulled into the mushroom cloud and spread in the local environment. In addition, the entirety of the H.M.S. Plym was vaporized except a few “red-hot fragments” that were thrown from the detonation site [16].

### ***Operation Hardtack***

Operations Hardtack is another set of 35 nuclear detonations at the Pacific Proving Grounds, including numerous surface water detonations. Table 2.1 shows a list and summary of details of the detonations relevant to marine debris formation.

**Table 2.1 Operation Hardtack Relevant Detonations**

Test	Height of Burst	Delivery	Purpose	Size
Butternut	3 m	Barge	Weapons Development (TX-46)	81 kt
Holly	4 m	Barge	Weapons Development (XW-31Y3)	5.9 kt
Nutmeg	3 m	Barge	Weapons Development	25.1 kt
Magnolia	4 m	Barge	Weapons Development (Cougar)	57 kt
Tobacco	2.7 m	Barge	Weapons Development (XW-50)	11.6 kt
Umbrella	-50 m	Underwater	Weapon Effect	8 kt
Linden	2.5 m	Barge	Weapons Development (XW-50)	11 kt
Hickory	3 m	Barge	Weapons Development (XW-47)	14 kt
Sequoia	2 m	Barge	Weapons Development (XW-50)	5.2 kt
Juniper	3 m	Barge	Weapons Development (XW-47)	65 kt

## ***Marine Debris Research***

The results from these weapons tests form the basis of the debris formation sections of Glasstone's *Effects of Nuclear Weapons*. In addition to results from the numerous weapon tests, research results from the 1960's provide insight into the possible debris expected in marine-urban debris. Freiling's 1962 work on the "Nature of Nuclear Debris in Sea-Water" provides a detailed summary of debris formation in purely marine environs [17]. The major aspects of this research relevant to this work is listed below.

- Shallow water detonations produce a smaller fireball than from a surface or air-burst.
- The duration of the shockwave is shorter in water detonations than in air detonations.
- Shallow water detonations produce craters that are wider (~10%) and shallower (~30%) than surface burst.
- For fully submerged detonations, all gasses and fission products rise in a bubble and are ejected once the bubble reaches the surface.
- The high humidity from the vaporized water produces a condensation cloud to form.
- The chalky sediment in the Marshall Island detonations produced calcareous coating on the water's surface and ships.
- Water detonations produce an estimated two ounces of fission products per kiloton detonation.
- In addition to water ion-activation, high induced activity in structural material such as zinc, copper, manganese, and iron are expected.
- Debris from water detonations is typically smaller and lighter than surface with less close in land fallout.

## **CHAPTER THREE**

### **ELEMENTAL CHARACTERIZATION OF MARINE-URBAN LAYERS**

To determine the predicted elemental components present in debris samples, it is first important to identify the extent to which the environmental and weapon device elements contribute to the composition of a debris sample. The composition set of elemental mass fractions present in the debris results from a combination of the set of environmental elementals ( $\bar{E}$ ) and elements present in the weapon fuel and components ( $\bar{W}$ ). The mass fractions of the elements in the detonation environment,  $\bar{T}$ , is then given by equation (3.1), where  $\omega_E$  and  $\omega_W$  are the mass fraction of environmental elements and weapon elements.

$$\bar{T} = \omega_E \bar{E} + \omega_W \bar{W} \quad (3.1)$$

A more detailed model expands the environmental variables into the specific layers: marine (M), soil (S), infrastructure (I), and vessels/vehicles (V).

$$\bar{T} = \omega_M \bar{E}_M + \omega_S \bar{E}_S + \omega_I \bar{E}_I + \omega_V \bar{E}_V + \omega_W \bar{W} \quad (3.2)$$

To determine the total debris mass fractions, it is essential to determine the mass fractions for each of the layers ( $\omega_k$ ), the set of mass fractions for each environmental layer ( $\bar{E}_k$ ), and the set of weapon mass fractions ( $\bar{W}$ ). The next sections will focus on each of these sets and variables.

### **Layer Mass Fraction Estimation**

The total elemental composition of the debris is dependent on the mass fraction of each layer consumed by the fireball, which is in turn dependent on the volume fraction of each layer. The size of the detonation's fireball provides a starting point to quantify the layer volume fractions. For surface detonations, the radius of the fireball ( $R_{fb}$  in meters) can be estimated using equation (3.3) [17].

$$R_{fb} = 27.432 Y^{0.4} \quad (3.3)$$

For an improvised nuclear device (IND) with a yield range of 5 to 15kT, this corresponded to a fireball radius of between about 52 and 81 meters. Using this fireball radius, we can examine the harbor environment to predict volume fractions. Figure 3.1 shows a representative image of a “Handy-size” shipping vessel in port with a 60-meter scale. This class of vessel has a length overall (LOA) of about 180-meters, a breadth of 30-meters, and a draft of 10-meters.



**Figure 3.1 Handy-size Shipping Vessel (60-Meter Scale)**

Since the Handy-size vessel represents the smallest commercial shipping vessel, we will utilize its dimensions to establish a lower limit for the vessel volume fraction and the upper limit for the water, soil, and infrastructure layers. The largest class of vessels that the Port of New York/New Jersey can currently facilitate has a LOA of about 350-meters, a breadth of 40-meters, and a draft of about 15-meters. This size of ship represents the upper limit on the volume fraction of the vessel layer and the lower fraction on the other layers for a NY/NJ detonation. Classes A through C in Figure 3.2 shows a brief summary of the dimensions of many of the possible vessels that the Port of NY/NJ can support.

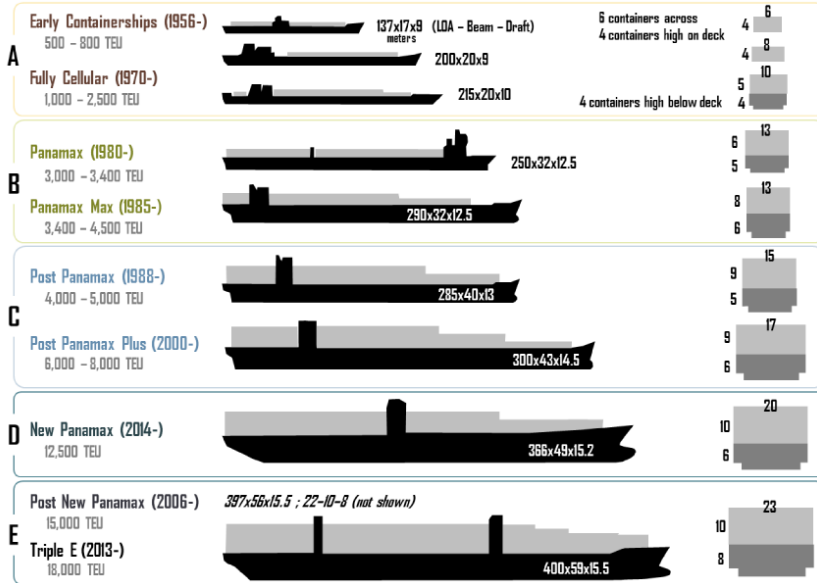


**Figure 3.2 Common Vessel Classes and Dimension [18]**

The Port of Los Angeles/Long Beach has a capacity for larger ships and routinely processes ships with LOA in excess of 350-meters and 50-meter widths. In addition, this port has a depth of over 52-meters. Class E ships represent the upper limit of ships utilized for modeling in the Port of LA/LB. The Port of Houston also regularly processes container-vessels with widths in excess of 40-meters. Moreover, the port primarily supports oil-tankers. These tankers can range in width from a minimum 30-meter (Handymax) to maximum 60-meters (Ultralarge Crude Carriers).

Because there are millions of possible combinations of ship sizes and port arrangements, we will examine a simplified model to describe the volume occupied by each layer in a detonation scenario. Figure 3.3 shows a 2D schematic of possible detonation scenarios. The red circles represent the fireball radii for 5 and 15kT yield detonations, while the two pentagons represent the minimum and maximum width and height for vessels. All layer volume calculations will be based on calculating the volume of the simplified shapes that make up this model.



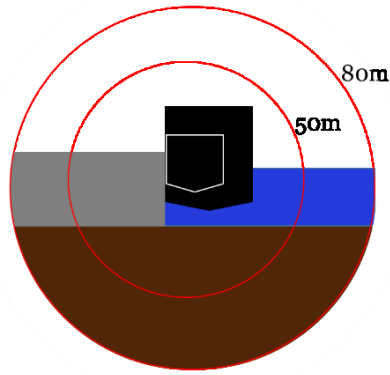


**Figure 3.3 2D Schematic of Fireball Environment and Layers**

### ***Vessel Layer Volume***

Representing the vessel as a simple parallelepiped, we can calculate the volume occupied with equation (3.4), where  $H_V$  and  $W_V$  are the effective height and width of the vessel and its contents, respectively. Because even the largest fireball radius is smaller than the length of the smallest vessel, the vessel length of concern will be limited by  $2R_{fb}$ .

$$V_V = 2R_{fb}H_VW_V \quad (3.4)$$

### ***Soil Layer Volume***

We will represent the soil layer as a spherical cap, which has the general volume equation below.

$$V = \pi/3 h^2(3r - h)$$

By assuming that the detonation occurs at the water's surface, the height/depth,  $h$ , of the cap is simply the fireball radius minus the depth of the water,  $H_M$ .

$$h = (R_{fb} - H_M)$$

The volume of the soil layer can then be found with equation (3.5) using the fireball radius and the water depth.

$$V_S = \frac{\pi}{3} (R - H_M)^2 (2R + H_M) \quad (3.5)$$

### ***Infrastructure Layer Volume***

The infrastructure layer can be represented as two distinct sublayers. The first sublayer is composed of the concrete and asphalt ground layer that provides support for the harbor. The second sublayer is composed of the vehicles and equipment necessary to operate the port. The volume of each of these sublayers can be calculated using a spherical segment approximation. Equation (3.6) represents the volume of the sublayer above the waterline, with  $H_{I,A}$  as the height of this layer above the water. Equation (3.7) is the volume of the sublayer with  $H_{I,U}$  as the height of the layer under the waterline.

$$V_{I,A} = \frac{\pi}{2} H_{I,A} \left( R^2 - \frac{H_{I,A}^2}{3} \right) \quad (3.6)$$

$$V_{I,U} = \frac{\pi}{2} H_{I,U} \left( R^2 - \frac{H_{I,U}^2}{3} \right) \quad (3.7)$$

### ***Marine Layer Volume***

A spherical segment approximation can also be used to calculate the volume of water in the fireball region. In (3.8),  $H_M$  represents the height/depth of this layer, which is the depth of the shipping channel. We also assume that 1/3 of the vessel's volume displaces the water volume with negligible rise in the channel depth.

$$V_M = \frac{\pi}{2} H_M \left( R^2 - \frac{H_M^2}{3} \right) - \frac{V_V}{3} \quad (3.8)$$

### ***Layer Void Fractions and Density***

While the above equations provide a reliable estimation of the volume occupied by each layer, these layers are not completely composed of solid matter. Each layer has a specific fraction of its volume occupied by air. For the ships, these voids make up the crew areas, walkways, cargo areas, and voids in cargo containers. The infrastructure layer has similar voids with the voids in shipping containers, structural buildings, and the vacant space between equipment such as cranes, and container lifts. Additionally, the concrete and asphalt base of this layer

will contain voids between particles. The soil layer will have similar voids due to the porosity of the layer.

While the water layer does not have voids in the same way that the other layers do, not all of the water's mass will be incorporated into the debris. Because of the low vapor pressure for H<sub>2</sub>O, it will largely remain as steam when debris nucleation commences. Similarly, the dissolved gasses will not have a role in debris formation. The total mass of the material available from the marine layer for nucleation only comes from the salts and the sediment. For the marine layer, we can think of the void fraction as the percentage of H<sub>2</sub>O, dissolved gasses, and other organic material that will not be incorporated into the debris. As such, only a small fraction of the marine layer will be included in the debris.

After accounting for the layer void-fractions, we can calculate the mass of each layer using the layers averaged density,  $\rho_k$ . Using these estimated void-fractions and densities, the effective debris mass of each layer is found using equation (3.9).

$$m_k = V_k \rho_k v_k \quad (3.9)$$

### ***Weapon Elemental Contributions***

For the weapon elemental contributions, variables of interest include the weapon's fuel type and mass  $M_{Fuel}$ , the Yield, the presence of a tamper. Previous analysis has demonstrated that the mass fraction of residual fuel in a post-detonation sample is proportional to the original fuel mass of the weapon, in kg, and inversely proportional to the yield, in kT [13].

$$m_{resid,fuel} = 2.67 \times 10^{-6} \frac{M_{Fuel}}{Y} \quad (3.10)$$

Additionally, the mass fraction of any tamper material can be calculated using (1.10) [13].

$$m_{tamp} = \frac{3.2 \times 10^{-4}}{Y} \quad (3.11)$$

### ***Calculating Layer Mass Fraction***

The mass fraction for each layer,  $\omega_k$ , can be calculated by dividing the mass of each layer, by the total mass of all layers (3.12).

$$\omega_k = \frac{m_k}{\sum_k m_k} \quad (3.12)$$

Once these mass fractions are calculated, it is necessary to determine the mass fraction by element in each of the environmental layers.

## **Elemental Characterization of Marine-Urban Layers**

### ***Marine Water and Sedimentation Layer***

One of the challenges in characterizing aquatic layers is variability. The composition of soils and urban structures typically remain consistent, whereas the elemental composition of estuarial waters (harbors and ports) can change hourly according to weather and human activity. To develop the realistic surrogate debris representative of a marine-urban detonation, it is important to understand the full variation in the water composition, including examining the variability of salinity, dissolved gases, sedimentation processes, and organic material content.

Natural water systems are inherently complex and contain a mixture of nearly every naturally occurring element. In examining the composition of water, it is important to establish a minimum threshold below which elements will not be considered. For the following analysis, we will utilize a threshold of 1ppm (0.001 ‰) to screen trace constituents.

Variability of the salinity of global seawater can range from 33 ‰ water to 37 ‰. For estuarial system, this salinity variation can be as wide as 20 ‰, and stratification in these systems can cause salinity to vary according to depth by as much as 5 ‰ [19]. Natural and human influences both affect salinity in water systems. Natural influences include freshwater flow, tidal stage, stratification of estuarine waters, watershed size, and rainfall. Human influences include dams and river diversions, land development, and wastewater discharges. Because of

the circulation and mixing of seawater, the ratio of chlorine ions to other ions remains relatively constant. Table 3.1 shows the ionic composition of seawater with a salinity of about 34 ‰, which corresponds to a Chlorinity of 19 ‰.

An examination of historic and real-time salinity data from several locations in the NY/NJ harbor area indicate that salinity is normally distributed with a mean of 27.7 ‰ and a standard deviation of 1.5 ‰ [20]. Salinity values for the Port of Los Angeles are more consistent with ocean salinity of 30-36 ‰. Salinity values for major areas in the Galveston Bay region are considerably lower at about 7 ‰ with about a 1 ‰ standard deviation [21]. Ion ratios to Cl<sup>-</sup> in Table 3.1 will be used to calculate the concentration of all the possible salts in the environment for a given salinity value.

**Table 3.1 Ionic Composition of Sea Water [19]**

<b>Ion</b>	<b><i>g/kg</i></b>	<b>% Salts</b>	<b>Ratio to Cl<sup>-</sup></b>
Cl <sup>-</sup>	18.98	55.04	1.00
Br <sup>-</sup>	0.065	0.19	3.425E-03
SO <sub>4</sub> <sup>--</sup>	2.649	7.68	1.396E-01
HCO <sub>3</sub> <sup>-</sup>	0.14	0.41	7.376E-03
H <sub>3</sub> BO <sub>3</sub>	0.026	0.07	1.370E-03
Mg <sup>++</sup>	1.272	3.69	6.702E-02
Ca <sup>++</sup>	0.4	1.16	2.107E-02
Sr <sup>++</sup>	0.013	0.04	6.85E-04
K <sup>+</sup>	0.38	1.10	2.00E-02
Na <sup>+</sup>	10.556	30.61	5.562E-01

All aquatic systems contain dissolved atmospheric gasses. Many factors control the amount of these gasses present in a water sample. Among them, water temperature and salinity dominate. Additionally, biological cycles can significantly affect dissolved gas content. The primary dissolved gasses include oxygen and nitrogen. Carbon dioxide is also prevalent; however, it is often found in the form of bicarbonate [19][22]. For the NY/NJ inner harbor area, dissolved

oxygen content is measured between about 5 and 6 mg/L [20]. Dissolved nitrogen content in the NY/NJ harbor has been measured at concentration less than 0.1 mg/L; however, this concentration falls below the cut-off criteria of 1ppm and will not be considered.

In addition to salts and dissolved gases, colloidal particulates are bottom sediments also present in estuary waters. Many factors control the variability of sedimentation in estuary systems. The mechanisms controlling sedimentation include waves and tidal influences, river-water flow, and the size of the estuary watershed. In addition to the natural processes that affect estuarial sediment, dredging of waterways can significantly alter the soil composition. In order to maintain safe navigation in waterways, periodic dredging is required [23]. The overall effect of removing this material is dredging reduces of some of the variability in the sediments deposited on the marine-bottom as well as organic material. Among the elements present in estuary systems are silicon, antimony, arsenic, cadmium, chromium, copper, lead, mercury, nickel, silver, and zinc. Table 3.2 lists the concentration of suspended sediments found in the NY/NJ harbor area [24].

**Table 3.2 Elemental Concentrations (ppm) for Sediment Metals [24]**

<b>Element</b>	<b>As</b>	<b>Cd</b>	<b>Cr</b>	<b>Cu</b>	<b>Pb</b>	<b>Ni</b>	<b>Ag</b>	<b>Zn</b>
Mean	12.18	1.68	67.99	118.07	100.01	28.73	2.35	215.87
SD	6.38	1.64	36.79	97.76	80.47	16.01	1.83	135.39

Organic material is present in estuarial systems as both plants and animals. Because of the dredging operations discussed above, the plant material will be negligible compared to other water-system components. Additionally, we assume that the high traffic nature of the port operations disrupts marine animal habitation. What organic material is present in the environment at the time of detonation will largely be volatilized and will remain dissociated until after the debris particulates have formed. These organics will have insignificant contribution to the composition of the nuclear debris.

### ***Marine Vessels and Vehicles***

Previous work determining elemental contributions to debris samples from urban vehicular layers is not appropriate for the marine environment. Because the NY/NJ estuary system is used for both commercial and recreation activities, many different types of vessels can be found. If we consider a detonation only at a cargo terminal, the major elemental contributions to the debris in the vehicular layer come from barges or container ships and their associated cargo. Using marinetraffic.com, real-time monitoring of many possible ports is possible. At any given time, users can examine the types of vessels present and each vessels gross tonnage (GT), deadweight (DWT), and dimensions. For the Elizabeth Marine Terminal in the NY/NJ harbor area, the average deadweight of ships at the terminal is about 70,000 metric tons with a standard deviation of about 38,000 metric tons.

The deadweight of a vessel is the total weight of all cargo, fuel, and crew and can be used to estimate the density of the ships material and the void fraction. The total weight of a ship is the sum of its deadweight and the empty weight of the vessel—its light displacement (LDT). Since the average ratio of DWT to LDT for cargo ships is 0.43 [25] an empirical estimate of a ships total weight from its deadweight can be found using (3.13). We can similarly calculate the effective density of the vessel using its mass and dimensions (3.14).

$$m_v = 1.43DWT \quad (3.13)$$

$$\rho'_v = \frac{1.43DWT}{L \times H \times W} \quad (3.14)$$

This density includes the mass the ships structural material as well as its cargo contents, some of which may be organic. The LTD of a vessel is almost entirely from steel. However, depending on a vessel's container loading capacity, the steel shipping containers or bulk bladders account for only about 10-20% of a ships deadweight. The remaining 80-90% of the DWT is unknown cargo. Further analysis is necessary to determine possible elemental characteristics of this remaining mass from a ship-to-ship basis. Figure 3.4 shows the balance of total

shipping by commodity for all US cargo. As an initial basis, we will assume that most of the cargo material is volatile and will not be incorporated in any bulk marine-urban debris samples. We will assume that the material that is not volatile will be mainly steel based.

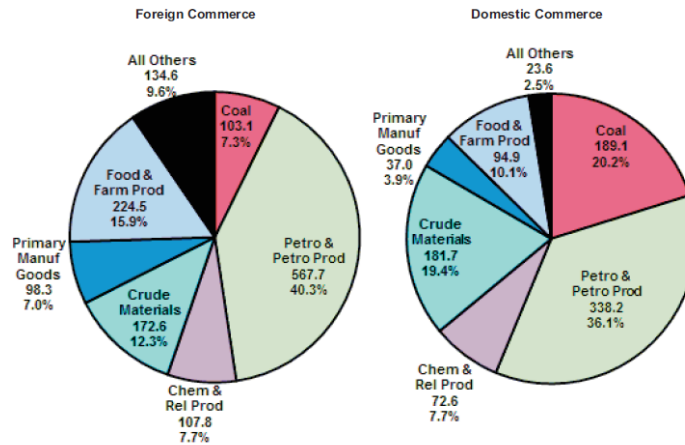


**Figure 3.4 Distribution of US Commerce by Commodity[26]**

For the weight fraction by element for steel, shipbuilding steel (AH32) is assumed for vessel steel and high strength steel is assumed for cargo containers. Using standard elemental composition for these materials [27][28], the elemental mass fractions from the steel for the vessel/vehicular layer are listed in Table 3.3.

**Table 3.3 Weight Percent for Vessel and Container Steel [27][28]**

Element	Fe	Mn	Ni	Si	Cr	Cu
Weight Percent	96.28	1.35	1.00	0.40	0.35	0.26
Element	C	Mo	S	P	Ti	Al
Weight Percent	0.20	0.06	0.04	0.036	0.015	0.01



### ***Soils and Infrastructure***

Since, previous work has developed the formulation for the surface concrete and soil layer in New York and Houston [13], this layers layer need not be developed here. However, the infrastructure layers for purely urban analysis focused on land use and building data. The infrastructure of a port area of operations typically contains a dense arrangement of steel storage containers on top of an asphalt and concrete surface, supported further by a structural layer of concrete. The remainder of the infrastructure in the port area of operations includes load-handling equipment such as cranes and forklifts. Since the majority of this equipment above ground is steel, we will use the elemental composition of high strength steel as the elemental composition of the above ground marine-urban infrastructure layer. Again further analysis of shipping container contents in necessary to more completely characterize this layer; nevertheless, we will assume the containers are either empty or contain materials that will not be incorporated into the bulk-debris.

The infrastructure sublayer under the surface is composed predominately of concrete. For the material properties of concrete, we will utilize the NIST reference composition for Portland cement and the material density of 2,300 kg/m<sup>3</sup> [29].

**Table 3.4 Elemental Weight Percent for Concrete (Portland) [29]**

<b>Element</b>	<b>H</b>	<b>C</b>	<b>O</b>	<b>Na</b>	<b>Mg</b>	<b>Al</b>	<b>Si</b>	<b>K</b>	<b>Ca</b>	<b>Fe</b>
Weight Percent	1.0	0.1	52.91	1.60	0.20	3.39	33.70	1.30	4.40	1.40

## Model Variable Inputs

A generalized composition of elements in a fireball can be calculated by discretizing the harbor regions into specific layers and analyzing the variable material in these layers that contribute to production of nuclear debris. In order to determine the range of expected compositions of marine-urban debris, a uniform yield range of 5-15kt will be utilized.

Table 3.5 shows a summary of the variables and their distribution that are used to develop model predictions of the marine-urban debris. In these models, harbor depths remain fixed and tidal fluctuations will be ignored [30].

**Table 3.5 Variable Distributions for the Port of Interest**

Variable	NY/NJ	Houston	LA/LB
Water/Soil Variables			
Salinity (g/kg)	N(27.5, 1.5)	N(7.0, 1.0)	N(33, 1.0)
Sediment (mg/kg)	N(5.4, 2.3)	N(3.0, 0.4)	N(1.2, 0.07)
Water Depth (m)	15	12	16
Soil Void Adjustment	U(0.66, 75)	U(0.66, 75)	U(0.66, 75)
Vehicle/Infrastructure Variables			
Vessel Width (meters)	U(30,40)	U(30,60)	U(30,60)
Vessel Void Adjustment	U(0.5, 0.65)	U(0.25,0.35)	U(0.5, 0.65)
Vessel Density(g/cm <sup>3</sup> )	U(7.75, 8.05)	U(7.75, 8.05)	U(7.75, 8.05)
Weapons Variables			
Yield (kt)	U(5, 15)		

## CHAPTER FOUR RESULTS AND DISCUSSION

### Calculated Layer Mass Fraction

Based on simple Monte-Carlo sampling (10,000 iterations) from the input distributions in Table 3.5, Table 4.1 shows the results of the calculated mass fraction for each of the layers, with the two components of the infrastructure layers combined. From Table 4.1, it is evident that the model inputs do provide different values for the layer mass fractions for each location. Specifically, we see that the Houston model has the lowest water and vessel fraction, with the highest soil fraction. Conversely, we see that the LA/LB model has the highest vessel mass fraction with the lowest soil contribution. The NY/NJ model has the highest water mass fraction and the highest mass contributions from infrastructure material.

**Table 4.1 Layer Mass Fraction for the Three Ports of Interest**

	NY/NJ	Houston	LA/LB
Marine Layer Mass Fraction	N(0.050, 0.005)	N(0.032, 0.011)	N(0.036, 0.012)
Soil Layer Mass Fraction	N(0.566, 0.069)	N(0.637, 0.085)	N(0.440, 0.098)
Vessel Layer Mass Fraction	N(0.340, 0.070)	N(0.283, 0.096)	N(0.488, 0.114)
Infrastructure Mass Fraction	N(0.045, 0.003)	N(0.024, 0.006)	N(0.035, 0.006)

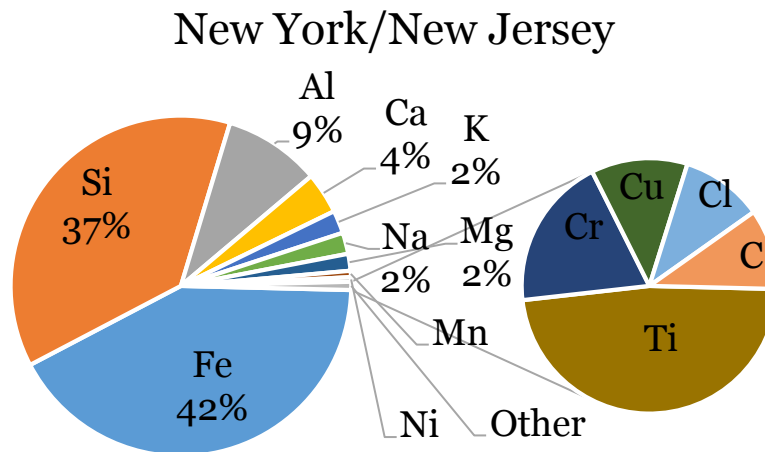
### Elemental Weight Percent for Marine Urban Debris

Table 4.2 provides a full list of the 26 elements and their associated mass fractions and the standard deviation of the mass fraction predicted by the model for each location.

**Table 4.2 Full Elemental Mass Fraction and Standard Deviation**

	NY/NJ		Houston		LB/LA	
	Mass Fraction	Standard Deviation	Mass Fraction	Standard Deviation	Mass Fraction	Standard Deviation
Fe	0.419	0.066	0.362	0.085	0.528	0.098
Si	0.373	0.045	0.412	0.058	0.298	0.066
Al	0.092	0.011	0.101	0.014	0.073	0.016
Ca	3.92E-02	4.70E-03	4.33E-02	6.10E-03	3.13E-02	7.00E-03
K	2.17E-02	2.60E-03	2.40E-02	3.39E-03	1.73E-02	3.90E-03
Na	2.02E-02	2.40E-03	2.20E-02	3.11E-03	1.62E-02	3.70E-03
Mg	1.60E-02	2.00E-03	1.77E-02	2.52E-03	1.28E-02	2.90E-03
Mn	6.00E-03	9.12E-04	5.24E-03	1.17E-03	7.50E-03	1.30E-03
Ni	4.30E-03	7.45E-04	3.65E-03	9.34E-04	5.40E-03	1.10E-03
Ti	3.70E-03	4.41E-04	4.11E-03	5.65E-04	3.00E-03	6.45E-04
Cr	1.50E-03	2.60E-04	1.26E-03	3.28E-04	1.90E-03	3.71E-04
Cu	9.45E-04	1.92E-04	7.71E-04	2.52E-04	1.30E-03	2.92E-04
Cl	8.03E-04	9.52E-05	1.30E-04	5.22E-05	7.26E-04	2.51E-04
C	7.88E-04	1.48E-04	6.60E-04	1.91E-04	1.00E-03	2.18E-04
P	7.42E-04	4.75E-05	7.84E-04	6.07E-05	6.65E-04	6.91E-05
S	5.56E-04	1.67E-05	5.38E-04	2.07E-05	5.28E-04	3.18E-05
Ba	3.61E-04	4.45E-05	4.00E-04	5.71E-05	2.88E-04	6.51E-05
Mo	2.17E-04	4.43E-05	1.77E-04	5.84E-05	2.94E-04	6.77E-05
Zn	1.14E-05	1.20E-06	7.26E-06	2.68E-06	8.58E-06	2.96E-06
Pb	5.27E-06	5.54E-07	3.36E-06	1.24E-06	3.97E-06	1.37E-06
Br	2.75E-06	3.26E-07	4.47E-07	1.79E-07	2.49E-06	8.61E-07
As	6.42E-07	6.75E-08	4.10E-07	1.51E-07	4.84E-07	1.67E-07
Sr	5.50E-07	6.52E-08	8.94E-08	3.58E-08	4.97E-07	1.72E-07
B	1.92E-07	2.28E-08	3.12E-08	1.25E-08	1.74E-07	6.02E-08
Ag	1.24E-07	1.30E-08	7.91E-08	2.92E-08	9.34E-08	3.22E-08
Cd	8.86E-08	9.31E-09	5.65E-08	2.09E-08	6.68E-08	2.30E-08

Figure 4.1 through 4.3 show a graphical representation of the predicted debris composition for each of the three port locations. Elements without a listed weight percent make up less than 1% of the debris. We can see from these figures and the results in Table 4.1 that the predicted debris is mostly a mix of iron and silicon.



**Figure 4.1 Elemental Composition of Predicted MUD for the Port of NY/NJ**

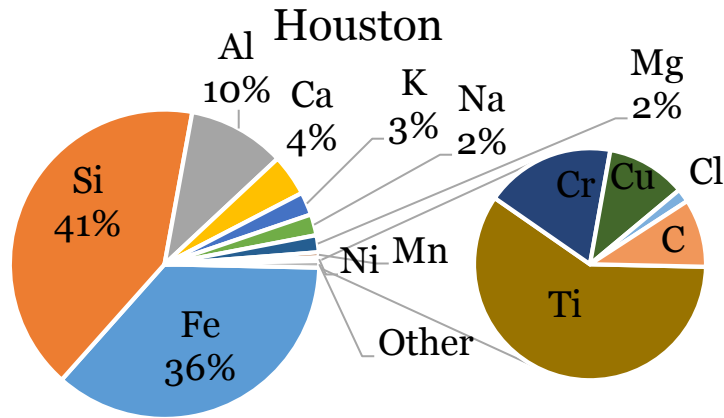


**Figure 4.2 Elemental Composition of Predicted MUD for the Houston Harbor**

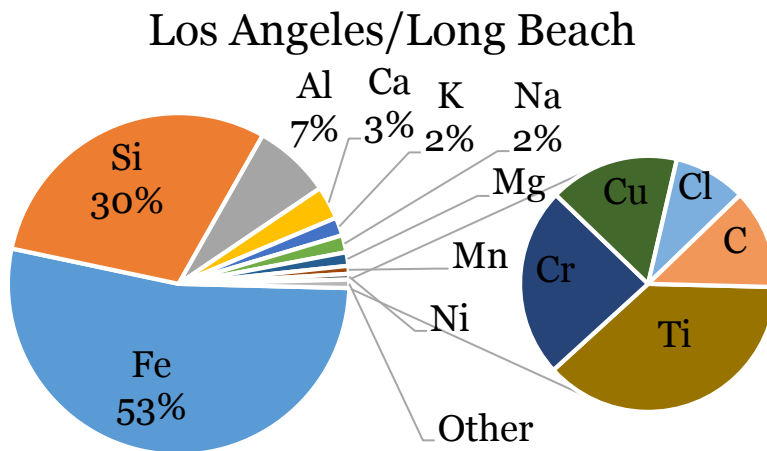


**Figure 4.3 Elemental Composition of Predicted MUD for the Port of LA/LB**

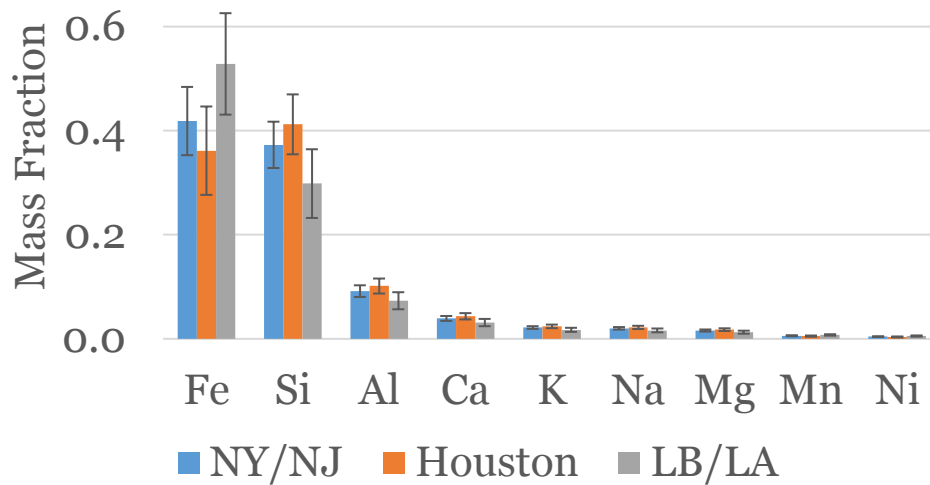


**Figure 4.4 Mass Fraction for Top Nine Elements by Location**

Figure 4.4 provides a graphical comparison of the mass fraction for the top nine elements by location. The error bars indicate one standard deviation. This figure also shows that the major elemental contributions predicted by the model include mostly iron and silicon with varying fractions by location. Results for NY/NJ near equal contributions from iron and silicon with a slightly higher concentration of iron. The Houston results indicate the opposite with higher silicon content than iron. Figure 4.1 also shows that the predicted iron content for LA/LB debris is considerably higher than the silicon content. Moreover, there is a slightly larger uncertainty in the iron and silicon content in the LA/LB model results.

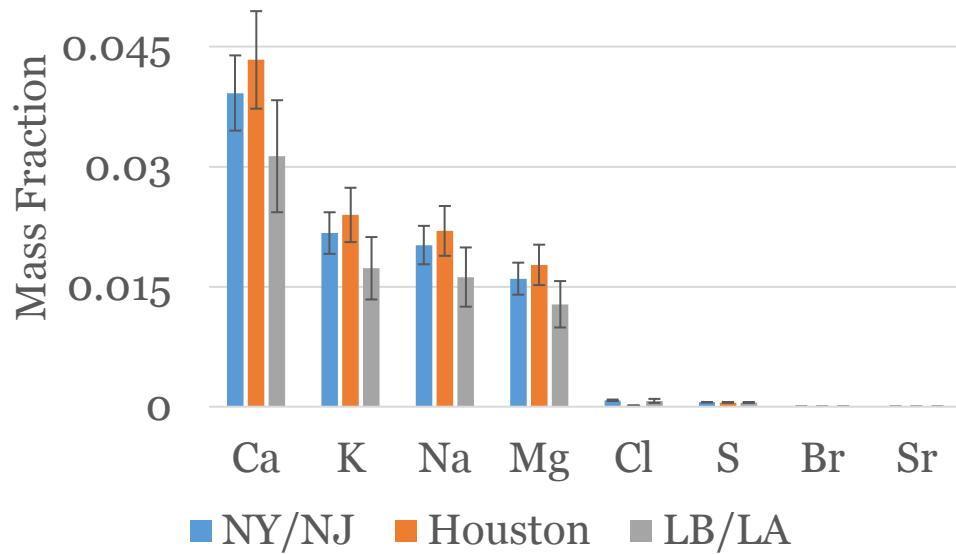


**Figure 4.5 Mass Fraction for Salts by Location**

Figure 4.5 shows the associated mass fractions for only the contributions from the salts in the environment. This figure shows that the predicted major salt contributions come mostly from calcium, potassium, sodium, and magnesium which are present at relatively high levels in soils and concrete, and present to a lesser extent in seawater. This indicates that the predicted salts in the debris come mainly from soil and infrastructure layers and not sea-salts. This will be examined further through a linear regression analysis of the variable contributions for each element.



## Oxide Powder Weight Percent for MUD Formulation

After determining the mass fraction for each element expected in the debris samples, it is next necessary to determine the mass fraction of the oxide powder mixes necessary to achieve the equivalent debris mass fraction. Using stoichiometric conversions, the oxide powder mass fractions required are listed in Table 4.3.

**Table 4.3 Oxide Powder Mass Fraction for each Location**

	SiO <sub>2</sub>	Fe <sub>2</sub> O <sub>3</sub>	Al <sub>2</sub> O <sub>3</sub>	CaO	KOH	NaOH
NYC	0.459	0.344	0.100	0.0316	0.0179	0.0202
Houston	0.497	0.292	0.108	0.0342	0.0194	0.0216
LB/LA	0.382	0.452	0.0828	0.0262	0.0149	0.0169
	MgO	O <sub>2</sub> Ti	MnO	Ca <sub>3</sub> (PO <sub>4</sub> ) <sub>2</sub>	SO <sub>2</sub>	Cr <sub>2</sub> O <sub>3</sub>
NYC	0.0153	0.00355	0.00446	0.00214	0.000639	0.00083
Houston	0.0166	0.00387	0.00382	0.00221	0.000606	0.000682
LB/LA	0.0127	0.00300	0.00580	0.00199	0.000632	0.00109

## Model and Variable Sensitivity Analysis

An important aspect of any model is the model's ability to produce significantly different results with different model inputs. While Figures 4.4 and 4.5 appear to demonstrate that the elemental composition for each location are different, it is important to examine if these differences are statistically significant. Analysis-of-variance (ANOVA) provides a method to determine statistically significant differences among the elemental mass fraction results for the three locations. For each element,  $i$ , we will test to determine if the mean elemental weight percent,  $\mu_i$ , are equal for the three locations. The null and alternate hypotheses are listed below.

$$\begin{aligned}
H_0: \mu_{i,NYNY} &= \mu_{i,HOU} = \mu_{i,LALB} \\
H_A: & \text{At least one } \mu_i \text{ is different}
\end{aligned}
\tag{4.1}$$

The statistical software package *Stata* provides a means to quickly compute the test statistic (F-Statistic) and p-values for these tests. The full results of running a one-way ANOVA test for each element are shown in Appendix A. Each of the 26 elements predicted by the model have p-values less than 0.01, indicating that the null-hypothesis should be rejected even at a 99% confidence level. For each element, the difference in mean mass fraction among the three locations are all statistically significant.

While the ANOVA results indicate that the model provides statistically significant results for each set of variables associated with each location, it is also important to determine to what extent each variable contributes to the overall mass fraction for each element. Because the model is a deterministic model, we can combine all of the layer volume and mass fraction equations with the inputs in Table 3.5 to determine variable sensitivities. However, these concocted equations have a mix of variable products, powers, and summations. A simple method for determining the effect of each variable is to use a simple linear model (4.2).

$$T_i = \beta_{i,1}Yield + \beta_{i,2}W_V + \beta_{i,3}H_M + \beta_{i,4}Salinity + \beta_{i,5}v_V \tag{4.2}$$

Performing multiple linear regression analysis for each of the  $i$  elements allows for the determination of the magnitude of each of the  $j$  variable contribution,  $\beta_{i,j}$ . The full results of this regression analysis with *Stata* can be found in Appendix B. For all 26 elements, the  $R^2$  value, which indicates how well the linear model fits the actual model data, is greater than 0.98. Such a high value indicates that the linear model (4.2) provides a very good fit for the actual model. Table 4.4 shows the linear model coefficients for the top ten elements predicted.

**Table 4.4 Linear Model Coefficients for Top Ten Elements**

	Yield	Salinity	Ship Width	Water Depth	Vessel Void Adjustment
Fe	-0.0173	-0.0008*	0.0078	0.0059	0.4283
Si	0.0119	-0.0076	-0.0054	0.0573	-0.3603
Al	0.0030	-0.0019	-0.0013	0.0141	-0.0893
Ca	0.0013	-0.0008	-0.0006	0.0061	-0.0382
K	0.0007	-0.0004	-0.0003	0.0033	-0.0212
Na	0.0006	-0.0004	-0.0003	0.0031	-0.0196
Mg	0.0053	-0.0003	-0.0002	0.0025	-0.0156
Mn	-0.0002	0.0000*	0.0001	0.0001	0.0059
Ni	-0.0002	0.0000*	0.0008	0.0001	0.0045
Ti	0.0001	-0.0001	-0.0001	0.0053	-0.0035

\*Not Statistically Significant at the 95% Confidence Level

By examining the sign and magnitude of the regression results, we can determine the partial effect of each variable in the overall model. Increasing the yield decreases the elemental mass fraction of the metals iron, manganese, and nickel, and increases the mass fraction for the remaining elements. In all cases, we see that this change varies between 1.73 percentage points and 0.01 percentage points for each 1-kt change in yield. For change in salinity, each additional g/kg of total salts in the marine water, the elemental composition for the top ten elements decreases. For iron, manganese, and nickel changes in salinity result in no statistically significant change in their mass fraction. These results indicate that overall, the composition of the seawater in the port/harbor has little effect on the overall composition of any predicted debris. The coefficients for ship width indicate that each additional ten meters of width results in a change in elemental weight percent between 7.8 (Fe) and 0.1 (Mn) percentage points. The most significant impact in changing water depth is a 5.7 percentage point increase in the

silicon weight percent for each additional one-meter of depth. Similar to *yield* and *salinity*, changes in the *vessel void adjustment* results in an increase in the iron, manganese, nickel content while decreasing the contributions from the other elements. Notably, a 0.1 increase in the vessel void adjustment (10% less void space) results in a 4.2 percentage point increase in the iron weight percent and a 3.6 percentage point decrease in the silicon weight percent.

### Ferrosilicon Production Challenges

The induction-furnace “baking” process has provided success with surrogate trinitite and urban surrogate debris; however, efforts to produce marine-urban debris with relatively high iron content have been less successful. Figure 4.6 show the results of six melts with varying mass fractions of iron. From these figures, we see that melts or ingots with an iron content of about 20-30% do not form in the furnace under these conditions.

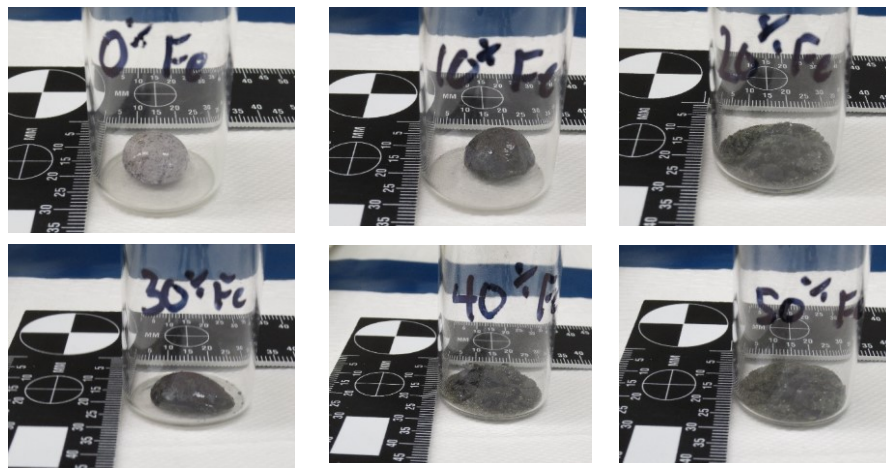


**Figure 4.6 Results of Melts/Ingots with Varying Fractions of Iron**

## **CHAPTER FIVE CONCLUSIONS AND RECOMMENDATIONS**

### **Conclusions**

This work demonstrates a unique methodology for predicting the elemental mass fraction of debris particulate found during the early stages of fireball formation in a nuclear detonation. Examination of the geometry of the detonation site provides an estimate of the volume fraction of each of the soil, water, vessel, and infrastructure layers. Using the averaged densities of this layer and layer liquid/water void adjustments, we can then determine the overall mass fraction of each layer. Finally, multiplying each layers mass fraction with the averaged elemental mass fractions for the layer produces the situation dependent elemental mass fraction for the early debris formation products. However, as discussed in Chapter 1, the complete debris formation process involves many complex physical processes, including radiological and environmental fractionation. Moreover, the elemental mass fractions determined in this work are pre-neutron activation results.

### **Future Work**

#### ***Neutron Activation***

To complete the work of developing realistic marine-urban debris surrogates, several future research efforts are necessary. Future work includes performing neutron activation analysis of the marine-urban environment to determine the composition of activation products and fission products produced. The Fallout-Analysis-Tool (FAT) developed at Oak-Ridge National Laboratory, provides a means of determining activation products (AP) and fission products (FP) from a detonation.

One of the shortfalls of this program is that it determines the AP and FP from a homogeneous mix of material. As demonstrated in Chapter 2, the material composition of the environment is heavily dependent on the geometry of detonation scenario. Monte Carlo N-Particle (MCNP) codes provide more utility for determining AP and FP because this code suite can account for the complex material composition and the geometries associated with a detonation scenario. This research effort should include building a set of MCNP models representative of the model inputs used in this research to determine the extent of FP and AP production as well as their sensitivity to the model input variables.

***Environmental Fractionation***

Fractionation studies must also be performed on the whole range of residual fuel elements, bulk environment elements, fission products, and activation products to determine which elements will be incorporated into debris matrices, and to what extent. As the fireball begins to cool, volatile and refractory elements will condense at different rates and be incorporated into the debris differently. Refractory elements will condense soonest and will have a higher concentration towards the inside of any debris. The volatile elements will condense later and will form towards the outside of the debris particles. Table 5.1 lists the refractory or volatility class for all elements predicted in the marine-urban-debris model.

**Table 5.1 Refractory and Volatile Elements for Marine-Urban-Debris**

Class	Elements
Volatile	Cl, Br, Cd, and Pb
Moderately Refractory	P, S, As, Cs, K, Na, Zn, Mn, Ag, and Cu
Refractory	Mg, Al, Ti, Ca, Sr, Ba, Si, Mo, Cr, Ni, and Fe

Table 5.1 demonstrates that the major components are refractory and will be incorporated into any debris; however, some of the elements are volatile and may not be incorporated as readily. Additionally, while Table 5.1 provides general classification, each element has different chemical properties that will effect debris formation. Future work should include research to determine the extent of these differences in elemental incorporation in debris particulates. Special attention should be paid to determining the extent of fractionation in the high humidity conditions of a marine detonation.

## **WORKS CITED**



- [1] DHS Press Office, “DHS Announces Expansion of the Securing the Cities Program.” DHS, Washington D.C., 2015.
- [2] J. Medalia, “CRS Report for Congress Received through the CRS Web Terrorist Nuclear Attacks on Seaports : Threat and Response,” 2005.
- [3] “Covering the Waterfront: A Review of Seaport Security Since September 11, 2001, Subcommittee on Terrorism, Technology, and Homeland Security,” 2004, pp. 1–67.
- [4] United States Maritime Administration, “Maritime Data & Statistics,” 2016. [Online]. Available: <http://www.marad.dot.gov/resources/data-statistics/>.
- [5] US Department of Transportation, “Freight Facts and Figures,” Washington D.C., 2013.
- [6] R. Stone, “Surprise Nuclear Strike? Here’s How We’ll Figure Out Who Did It,” *Science (New York, N.Y.)*, Mar-2016.
- [7] A. J. Fahey, C. J. Zeissler, D. E. Newbury, J. Davis, and R. M. Lindstrom, “Postdetonation Nuclear Debris for Attribution.,” *Proc. Natl. Acad. Sci. U. S. A.*, vol. 107, no. 47, pp. 20207–12, Nov. 2010.
- [8] P. Pease, “Fused Glass Sample Preparation for Quantitative Laser-Induced Breakdown Spectroscopy of Geologic Materials,” *Spectrochim. Acta - Part B At. Spectrosc.*, vol. 83–84, pp. 37–49, 2013.
- [9] K. P. Carney, M. R. Finck, C. A. McGrath, L. R. Martin, and R. R. Lewis, “The Development of Radioactive Glass Surrogates for Fallout Debris,” *J. Radioanal. Nucl. Chem.*, vol. 299, no. 1, pp. 363–372, 2014.
- [10] A. C. Pierre, *Introduction to Sol-Gel Processing*. New York, NY: Springer Science and Business Media, LLC, 2002.
- [11] J. J. Molgaard, “Production of Nuclear Debris Surrogates for Forensic Methods Development,” The University of Tennessee, 2014.

- [12] J. J. Molgaard, J. D. Auxier, A. V. Giminaro, C. J. Oldham, M. T. Cook, S. A. Young, and H. L. Hall, "Development of Synthetic Nuclear Melt Glass for Forensic Analysis," *J. Radioanal. Nucl. Chem.*, vol. 304, no. 3, pp. 1293–1301, 2015.
- [13] A. V. Giminaro, S. A. Stratz, J. a. Gill, J. P. Auxier, C. J. Oldham, M. T. Cook, J. D. Auxier, J. J. Molgaard, and H. L. Hall, "Compositional planning for development of synthetic urban nuclear melt glass," *J. Radioanal. Nucl. Chem.*, vol. 306, no. 1, pp. 175–181, 2015.
- [14] "Historical Report Atomic Bomb Tests Able and Baker (Operation Crossroads)," 1946.
- [15] "Operation Crossroads: Official Report," Washington D.C., 1946.
- [16] "Operation Hurricane."
- [17] S. Glasstone and P. Dolan, *The Effects of Nuclear Weapons*, 3rd ed. Washington D.C.: U.S. Government Printing Office, 1977.
- [18] "Ship Size Info." [Online]. Available: <http://www.nextbigfuture.com/2014/10/container-ship-almost-twice-as-long-as.html>.
- [19] C. Chen, "General Chemistry of Sea Water," *Encycropedia Life Support Syst.*, 2006.
- [20] US Geological Surveys, "Water Data for New York," 2016. [Online]. Available: <http://waterdata.usgs.gov/ny/nwis>.
- [21] "NOAA Data Houston." [Online]. Available: [https://tidesandcurrents.noaa.gov/ofs/ngofs/ngofs\\_galveston.html](https://tidesandcurrents.noaa.gov/ofs/ngofs/ngofs_galveston.html).
- [22] Science Learning Hub, "Ocean dissolved gases," 2010. [Online]. Available: <http://sciencelearn.org.nz/Contexts/The-Ocean-in-Action/Science-Ideas-and-Concepts/Ocean-dissolved-gases>.

- [23] New York/New Jersey Harbor Estuary Program, "Regional Sediment Management Plan," New York, NY, 2008.
- [24] "Contaminant Assessment and Reduction Project : NY / NJ Harbor Sediment Report," New York, NY, 2003.
- [25] M. Lutzen and H. O. Kristensen, "Statistical Analysis and Determination of Regression Formulas for Main Dimensions of Container Ships Based on IHS Fairplay Data," Denmark, 2013.
- [26] "Waterborne Commerce of the United States," Alexandria, VA, 2014.
- [27] Total Materia, "Shipbuilding Steels: Part One," 2010. [Online]. Available: <http://www.totalmateria.com/page.aspx?ID=CheckArticle&site=kts&NM=287>.
- [28] MatWeb, "ASTM A131 Steel, Grade AH32 Datasheet," *Material Property Data*. [Online]. Available: <http://www.matweb.com/search/datasheet.aspx?matguid=3e5a3d6e35e04f9e96a98f2c9cfo488c&ckck=1>.
- [29] "NIST Portland Cement." [Online]. Available: <http://physics.nist.gov/cgi-bin/Star/compos.pl?matno=144>.
- [30] J.-P. Rodrigue, "The Geography of Transport Systems," *Hofstra University, Department of Global Studies and Geography*, 2016. [Online]. Available: <https://people.hofstra.edu/geotrans/eng/ch4en/conc4en/uswaterwaysystem.html>.

## **APPENDIX**

## APPENDIX A: STATA ANOVA Results

. oneway B loc

Analysis of Variance					
Source	SS	df	MS	F	Prob > F
Between groups	1.4998e-12	2	7.4990e-13	565.13	0.0000
Within groups	3.9411e-13	297	1.3270e-15		
Total	1.8939e-12	299	6.3341e-15		

Bartlett's test for equal variances:  $\chi^2(2) = 220.1013$  Prob> $\chi^2 = 0.000$

. oneway C loc

Analysis of Variance					
Source	SS	df	MS	F	Prob > F
Between groups	7.5534e-06	2	3.7767e-06	125.99	0.0000
Within groups	8.9026e-06	297	2.9975e-08		
Total	.000016456	299	5.5037e-08		

Bartlett's test for equal variances:  $\chi^2(2) = 14.0504$  Prob> $\chi^2 = 0.001$

.  
. oneway Na loc

Analysis of Variance					
Source	SS	df	MS	F	Prob > F
Between groups	.001863115	2	.000931558	113.73	0.0000
Within groups	.002432768	297	8.1911e-06		
Total	.004295884	299	.000014368		

Bartlett's test for equal variances:  $\chi^2(2) = 16.5528$  Prob> $\chi^2 = 0.000$

. oneway Mg loc

Analysis of Variance					
Source	SS	df	MS	F	Prob > F
Between groups	.001311063	2	.000655532	124.35	0.0000
Within groups	.00156566	297	5.2716e-06		
Total	.002876723	299	9.6211e-06		

Bartlett's test for equal variances:  $\chi^2(2) = 14.0766$  Prob> $\chi^2 = 0.001$

.  
. oneway Si loc

Analysis of Variance					
Source	SS	df	MS	F	Prob > F
Between groups	.702583725	2	.351291862	128.56	0.0000
Within groups	.811581359	297	.002732597		
Total	1.51416508	299	.005064097		

Bartlett's test for equal variances:  $\chi^2(2) = 14.6868$  Prob> $\chi^2 = 0.001$

. oneway Fe loc

Source	Analysis of Variance			F	Prob > F
	SS	df	MS		
Between groups	1.50952225	2	.754761123	126.68	0.0000
Within groups	1.76954716	297	.005958071		
Total	3.27906941	299	.010966787		

Bartlett's test for equal variances: chi2(2) = 14.8153 Prob>chi2 = 0.001

. oneway P loc

Source	Analysis of Variance			F	Prob > F
	SS	df	MS		
Between groups	7.6613e-07	2	3.8307e-07	126.42	0.0000
Within groups	8.9997e-07	297	3.0302e-09		
Total	1.6661e-06	299	5.5723e-09		

Bartlett's test for equal variances: chi2(2) = 13.2209 Prob>chi2 = 0.001

. oneway S loc

Source	Analysis of Variance			F	Prob > F
	SS	df	MS		
Between groups	4.5299e-08	2	2.2649e-08	45.76	0.0000
Within groups	1.4700e-07	297	4.9495e-10		
Total	1.9230e-07	299	6.4314e-10		

Bartlett's test for equal variances: chi2(2) = 44.6514 Prob>chi2 = 0.000

. oneway Cl loc

Source	Analysis of Variance			F	Prob > F
	SS	df	MS		
Between groups	.000026143	2	.000013071	565.13	0.0000
Within groups	6.8696e-06	297	2.3130e-08		
Total	.000033013	299	1.1041e-07		

Bartlett's test for equal variances: chi2(2) = 220.1013 Prob>chi2 = 0.000

. oneway K loc

Source	Analysis of Variance			F	Prob > F
	SS	df	MS		
Between groups	.002417501	2	.001208751	127.29	0.0000
Within groups	.002820368	297	9.4962e-06		
Total	.005237869	299	.000017518		

Bartlett's test for equal variances: chi2(2) = 14.4018 Prob>chi2 = 0.001

. oneway Ca loc

Analysis of Variance

Source	SS	df	MS	F	Prob > F
Between groups	.007896392	2	.003948196	128.81	0.0000
Within groups	.009103502	297	.000030652		
Total	.016999895	299	.000056856		

Bartlett's test for equal variances:  $\chi^2(2) = 14.9911$  Prob> $\chi^2 = 0.001$

. oneway Ti loc

Analysis of Variance					
Source	SS	df	MS	F	Prob > F
Between groups	.000066452	2	.000033226	126.15	0.0000
Within groups	.000078224	297	2.6338e-07		
Total	.000144676	299	4.8387e-07		

Bartlett's test for equal variances:  $\chi^2(2) = 13.5763$  Prob> $\chi^2 = 0.001$

. oneway Cr loc

Analysis of Variance					
Source	SS	df	MS	F	Prob > F
Between groups	.000021318	2	.000010659	120.31	0.0000
Within groups	.000026314	297	8.8599e-08		
Total	.000047632	299	1.5931e-07		

Bartlett's test for equal variances:  $\chi^2(2) = 11.6998$  Prob> $\chi^2 = 0.003$

. oneway Mn loc

Analysis of Variance					
Source	SS	df	MS	F	Prob > F
Between groups	.000285335	2	.000142667	125.41	0.0000
Within groups	.000337863	297	1.1376e-06		
Total	.000623198	299	2.0843e-06		

Bartlett's test for equal variances:  $\chi^2(2) = 14.2468$  Prob> $\chi^2 = 0.001$

. oneway Fe loc

Analysis of Variance					
Source	SS	df	MS	F	Prob > F
Between groups	1.50952225	2	.754761123	126.68	0.0000
Within groups	1.76954716	297	.005958071		
Total	3.27906941	299	.010966787		

Bartlett's test for equal variances:  $\chi^2(2) = 14.8153$  Prob> $\chi^2 = 0.001$

. oneway Ni loc

Analysis of Variance					
Source	SS	df	MS	F	Prob > F
Between groups	.0001711	2	.00008555	118.72	0.0000
Within groups	.000214023	297	7.2062e-07		

```
-----
Total          .000385123    299    1.2880e-06
Bartlett's test for equal variances:  chi2(2) = 11.3344  Prob>chi2 = 0.003
```

```
. oneway Cu loc
```

Analysis of Variance					
Source	SS	df	MS	F	Prob > F
Between groups	.000013941	2	6.9707e-06	132.71	0.0000
Within groups	.0000156	297	5.2527e-08		
Total	.000029542	299	9.8802e-08		

```
Bartlett's test for equal variances:  chi2(2) = 16.8033  Prob>chi2 = 0.000
```

```
. oneway Zn loc
```

Analysis of Variance					
Source	SS	df	MS	F	Prob > F
Between groups	9.6164e-10	2	4.8082e-10	89.25	0.0000
Within groups	1.6001e-09	297	5.3874e-12		
Total	2.5617e-09	299	8.5675e-12		

```
Bartlett's test for equal variances:  chi2(2) = 73.8302  Prob>chi2 = 0.000
```

```
. oneway As loc
```

Analysis of Variance					
Source	SS	df	MS	F	Prob > F
Between groups	3.0614e-12	2	1.5307e-12	89.25	0.0000
Within groups	5.0938e-12	297	1.7151e-14		
Total	8.1553e-12	299	2.7275e-14		

```
Bartlett's test for equal variances:  chi2(2) = 73.8302  Prob>chi2 = 0.000
```

```
. oneway Br loc
```

Analysis of Variance					
Source	SS	df	MS	F	Prob > F
Between groups	3.0667e-10	2	1.5334e-10	565.13	0.0000
Within groups	8.0585e-11	297	2.7133e-13		
Total	3.8726e-10	299	1.2952e-12		

```
Bartlett's test for equal variances:  chi2(2) = 220.1013  Prob>chi2 = 0.000
```

```
. oneway Sr loc
```

Analysis of Variance					
Source	SS	df	MS	F	Prob > F
Between groups	1.2267e-11	2	6.1334e-12	565.13	0.0000
Within groups	3.2234e-12	297	1.0853e-14		
Total	1.5490e-11	299	5.1807e-14		



Bartlett's test for equal variances:  $\chi^2(2) = 220.1013$  Prob> $\chi^2 = 0.000$

. oneway Mo loc

Analysis of Variance					
Source	SS	df	MS	F	Prob > F
Between groups	7.4186e-07	2	3.7093e-07	131.48	0.0000
Within groups	8.3788e-07	297	2.8212e-09		
Total	1.5797e-06	299	5.2834e-09		

Bartlett's test for equal variances:  $\chi^2(2) = 17.0882$  Prob> $\chi^2 = 0.000$

.  
. oneway Ag loc

Analysis of Variance					
Source	SS	df	MS	F	Prob > F
Between groups	1.1396e-13	2	5.6981e-14	89.25	0.0000
Within groups	1.8962e-13	297	6.3845e-16		
Total	3.0358e-13	299	1.0153e-15		

Bartlett's test for equal variances:  $\chi^2(2) = 73.8302$  Prob> $\chi^2 = 0.000$

. oneway Cd loc

Analysis of Variance					
Source	SS	df	MS	F	Prob > F
Between groups	5.8243e-14	2	2.9122e-14	89.25	0.0000
Within groups	9.6910e-14	297	3.2630e-16		
Total	1.5515e-13	299	5.1891e-16		

Bartlett's test for equal variances:  $\chi^2(2) = 73.8302$  Prob> $\chi^2 = 0.000$

.  
. oneway Ba loc

Analysis of Variance					
Source	SS	df	MS	F	Prob > F
Between groups	6.7732e-07	2	3.3866e-07	126.29	0.0000
Within groups	7.9643e-07	297	2.6816e-09		
Total	1.4737e-06	299	4.9289e-09		

Bartlett's test for equal variances:  $\chi^2(2) = 13.6598$  Prob> $\chi^2 = 0.001$

. oneway Pb loc

Analysis of Variance					
Source	SS	df	MS	F	Prob > F
Between groups	2.0640e-10	2	1.0320e-10	89.25	0.0000
Within groups	3.4343e-10	297	1.1563e-12		
Total	5.4983e-10	299	1.8389e-12		

Bartlett's test for equal variances:  $\chi^2(2) = 73.8302$  Prob> $\chi^2 = 0.000$

## APPENDIX B: STATA Regression Results

. regress B yield salinity ship\_W water\_D ves\_void, noconstant

Source	SS	df	MS	Number of obs	=	
Model	6.7686e-12	5	1.3537e-12	F(5, 295)	=	3145.61
Residual	1.2695e-13	295	4.3035e-16	Prob > F	=	0.0000
				R-squared	=	0.9816
				Adj R-squared	=	0.9813
Total	6.8955e-12	300	2.2985e-14	Root MSE	=	2.1e-08

B	Coef.	Std. Err.	t	P> t	[95% Conf. Interval]	
yield	8.34e-10	4.06e-10	2.05	0.041	3.47e-11	1.63e-09
salinity	4.27e-09	4.66e-10	9.17	0.000	3.35e-09	5.19e-09
ship_W	-4.43e-09	1.46e-10	-30.34	0.000	-4.72e-09	-4.14e-09
water_D	1.90e-08	8.48e-10	22.35	0.000	1.73e-08	2.06e-08
ves_void	-1.17e-07	3.22e-08	-3.63	0.000	-1.80e-07	-5.36e-08

. regress C yield salinity ship\_W water\_D ves\_void, noconstant

Source	SS	df	MS	Number of obs	=	
Model	.000222246	5	.000044449	F(5, 295)	=	34965.95
Residual	3.7501e-07	295	1.2712e-09	Prob > F	=	0.0000
				R-squared	=	0.9983
				Adj R-squared	=	0.9983
Total	.000222621	300	7.4207e-07	Root MSE	=	3.6e-05

C	Coef.	Std. Err.	t	P> t	[95% Conf. Interval]	
yield	-.0000393	6.98e-07	-56.25	0.000	-.0000407	-.0000379
salinity	-4.89e-08	8.00e-07	-0.06	0.951	-1.62e-06	1.53e-06
ship_W	.0000173	2.51e-07	69.10	0.000	.0000169	.0000178
water_D	3.32e-07	1.46e-06	0.23	0.820	-2.54e-06	3.20e-06
ves_void	.0009696	.0000553	17.52	0.000	.0008607	.0010785

. regress Na yield salinity ship\_W water\_D ves\_void, noconstant

Source	SS	df	MS	Number of obs	=	
Model	.1172775	5	.0234555	F(5, 295)	=	35976.20
Residual	.000192332	295	6.5197e-07	Prob > F	=	0.0000
				R-squared	=	0.9984
				Adj R-squared	=	0.9983
Total	.117469832	300	.000391566	Root MSE	=	.00081

Na	Coef.	Std. Err.	t	P> t	[95% Conf. Interval]	
yield	.0006429	.0000158	40.65	0.000	.0006117	.000674
salinity	-.0003952	.0000181	-21.80	0.000	-.0004309	-.0003595
ship_W	-.0003002	5.69e-06	-52.80	0.000	-.0003114	-.000289
water_D	.0030948	.000033	93.75	0.000	.0030299	.0031598
ves_void	-.0195729	.0012532	-15.62	0.000	-.0220392	-.0171066

. regress Mg yield salinity ship\_W water\_D ves\_void, noconstant

Source	SS	df	MS	Number of obs	=	
					=	300

-----				F(5, 295)	=	36003.63
Model		.074844295	5	.014968859	Prob > F	= 0.0000
Residual		.000122649	295	4.1576e-07	R-squared	= 0.9984
-----				Adj R-squared	=	0.9983
Total		.074966944	300	.00024989	Root MSE	= .00064

Mg		Coef.	Std. Err.	t	P> t	[95% Conf. Interval]
yield		.000529	.0000126	41.89	0.000	.0005042 .0005539
salinity		-.0003254	.0000145	-22.48	0.000	-.0003539 -.0002969
ship_W		-.0002355	4.54e-06	-51.87	0.000	-.0002444 -.0002266
water_D		.0024628	.0000264	93.42	0.000	.0024109 .0025146
ves_void		-.0156351	.0010007	-15.62	0.000	-.0176046 -.0136657

. regress Al yield salinity ship\_W water\_D ves\_void, noconstant

-----				Number of obs	=	300
-----				F(5, 295)	=	36178.19
Model		2.44587666	5	.489175331	Prob > F	= 0.0000
Residual		.003988776	295	.000013521	R-squared	= 0.9984
-----				Adj R-squared	=	0.9983
Total		2.44986543	300	.008166218	Root MSE	= .00368

Al		Coef.	Std. Err.	t	P> t	[95% Conf. Interval]
yield		.0030052	.0000072	41.73	0.000	.0028635 .0031469
salinity		-.0018727	.0000826	-22.68	0.000	-.0020352 -.0017102
ship_W		-.0013412	.0000259	-51.80	0.000	-.0013922 -.0012903
water_D		.0140942	.0001503	93.75	0.000	.0137984 .0143901
ves_void		-.0893234	.005707	-15.65	0.000	-.1005549 -.0780918

. regress Si yield salinity ship\_W water\_D ves\_void, noconstant

-----				Number of obs	=	300
-----				F(5, 295)	=	36863.63
Model		40.437474	5	8.0874948	Prob > F	= 0.0000
Residual		.064719912	295	.00021939	R-squared	= 0.9984
-----				Adj R-squared	=	0.9984
Total		40.5021939	300	.135007313	Root MSE	= .01481

Si		Coef.	Std. Err.	t	P> t	[95% Conf. Interval]
yield		.0119175	.0002901	41.08	0.000	.0113466 .0124884
salinity		-.0076052	.0003325	-22.87	0.000	-.0082596 -.0069507
ship_W		-.0054062	.0001043	-51.83	0.000	-.0056115 -.005201
water_D		.0572781	.0006055	94.59	0.000	.0560864 .0584699
ves_void		-.3602738	.0229882	-15.67	0.000	-.4055155 -.315032

. regress P yield salinity ship\_W water\_D ves\_void, noconstant

-----				Number of obs	=	300
-----				F(5, 295)	=	78575.27
Model		.000161386	5	.000032277	Prob > F	= 0.0000
Residual		1.2118e-07	295	4.1078e-10	R-squared	= 0.9992
-----				Adj R-squared	=	0.9992
Total		.000161507	300	5.3836e-07	Root MSE	= 2.0e-05

	P	Coef.	Std. Err.	t	P> t	[95% Conf. Interval]	
yield		.0000129	3.97e-07	32.55	0.000	.0000121	.0000137
salinity		-.0000123	4.55e-07	-26.96	0.000	-.0000132	-.0000114
ship_W		-5.67e-06	1.43e-07	-39.72	0.000	-5.95e-06	-5.39e-06
water_D		.0000922	8.29e-07	111.29	0.000	.0000906	.0000938
ves_void		-.0004113	.0000315	-13.08	0.000	-.0004732	-.0003494

. regress S yield salinity ship\_W water\_D ves\_void, noconstant

Source	SS	df	MS	Number of obs	=	300
Model	.000087629	5	.000017526	F(5, 295)	>	99999.00
Residual	4.5095e-08	295	1.5286e-10	Prob > F	=	0.0000
				R-squared	=	0.9995
				Adj R-squared	=	0.9995
Total	.000087674	300	2.9225e-07	Root MSE	=	1.2e-05

S	Coef.	Std. Err.	t	P> t	[95% Conf. Interval]	
yield	4.29e-06	2.42e-07	17.72	0.000	3.81e-06	4.77e-06
salinity	-6.56e-06	2.78e-07	-23.62	0.000	-7.10e-06	-6.01e-06
ship_W	-2.68e-06	8.71e-08	-30.74	0.000	-2.85e-06	-2.51e-06
water_D	.0000592	5.05e-07	117.09	0.000	.0000582	.0000602
ves_void	-.000181	.0000192	-9.43	0.000	-.0002188	-.0001432

. regress Cl yield salinity ship\_W water\_D ves\_void, noconstant

Source	SS	df	MS	Number of obs	=	300
Model	.000117982	5	.000023596	F(5, 295)	=	3145.61
Residual	2.2129e-06	295	7.5014e-09	Prob > F	=	0.0000
				R-squared	=	0.9816
				Adj R-squared	=	0.9813
Total	.000120195	300	4.0065e-07	Root MSE	=	8.7e-05

Cl	Coef.	Std. Err.	t	P> t	[95% Conf. Interval]	
yield	3.48e-06	1.70e-06	2.05	0.041	1.45e-07	6.82e-06
salinity	.0000178	1.94e-06	9.17	0.000	.000014	.0000217
ship_W	-.0000185	6.10e-07	-30.34	0.000	-.0000197	-.0000173
water_D	.0000791	3.54e-06	22.35	0.000	.0000722	.0000861
ves_void	-.0004884	.0001344	-3.63	0.000	-.000753	-.0002239

. regress K yield salinity ship\_W water\_D ves\_void, noconstant

Source	SS	df	MS	Number of obs	=	300
Model	.136512577	5	.027302515	F(5, 295)	=	36203.05
Residual	.000222474	295	7.5415e-07	Prob > F	=	0.0000
				R-squared	=	0.9984
				Adj R-squared	=	0.9983
Total	.136735052	300	.000455784	Root MSE	=	.00087

K	Coef.	Std. Err.	t	P> t	[95% Conf. Interval]	
yield	.0007057	.000017	41.49	0.000	.0006722	.0007392
salinity	-.0004425	.0000195	-22.70	0.000	-.0004809	-.0004042
ship_W	-.0003175	6.12e-06	-51.93	0.000	-.0003296	-.0003055
water_D	.0033359	.0000355	93.96	0.000	.003266	.0034058
ves_void	-.0211272	.0013478	-15.68	0.000	-.0237798	-.0184747

```
. regress Ca yield salinity ship_W water_D ves_void, noconstant
```

Source	SS	df	MS	Number of obs	=	300
Model	.44625168	5	.089250336	F(5, 295)	=	36391.64
Residual	.000723486	295	2.4525e-06	Prob > F	=	0.0000
				R-squared	=	0.9984
				Adj R-squared	=	0.9984
Total	.446975166	300	.001489917	Root MSE	=	.00157

Ca	Coef.	Std. Err.	t	P> t	[95% Conf. Interval]
yield	.0012567	.0000307	40.97	0.000	.0011964 .0013171
salinity	-.0008025	.0000352	-22.83	0.000	-.0008717 -.0007334
ship_W	-.0005744	.000011	-52.09	0.000	-.0005961 -.0005527
water_D	.0060508	.000064	94.51	0.000	.0059248 .0061768
ves_void	-.0382182	.0024305	-15.72	0.000	-.0430016 -.0334348

```
. regress Ti yield salinity ship_W water_D ves_void, noconstant
```

Source	SS	df	MS	Number of obs	=	300
Model	.00404421	5	.000808842	F(5, 295)	=	38057.50
Residual	6.2697e-06	295	2.1253e-08	Prob > F	=	0.0000
				R-squared	=	0.9985
				Adj R-squared	=	0.9984
Total	.004050479	300	.000013502	Root MSE	=	.00015

Ti	Coef.	Std. Err.	t	P> t	[95% Conf. Interval]
yield	.000119	2.86e-06	41.66	0.000	.0001133 .0001246
salinity	-.0000748	3.27e-06	-22.86	0.000	-.0000813 -.0000684
ship_W	-.0000524	1.03e-06	-51.04	0.000	-.0000544 -.0000504
water_D	.0005629	5.96e-06	94.44	0.000	.0005511 .0005746
ves_void	-.0035045	.0002263	-15.49	0.000	-.0039498 -.0030592

```
. regress Cr yield salinity ship_W water_D ves_void, noconstant
```

Source	SS	df	MS	Number of obs	=	300
Model	.000759211	5	.000151842	F(5, 295)	=	39529.57
Residual	1.1332e-06	295	3.8412e-09	Prob > F	=	0.0000
				R-squared	=	0.9985
				Adj R-squared	=	0.9985
Total	.000760344	300	2.5345e-06	Root MSE	=	6.2e-05

Cr	Coef.	Std. Err.	t	P> t	[95% Conf. Interval]
yield	-.0000699	1.21e-06	-57.61	0.000	-.0000723 -.0000675
salinity	-2.52e-06	1.39e-06	-1.81	0.071	-5.26e-06 2.14e-07
ship_W	.0000289	4.36e-07	66.17	0.000	.000028 .0000297
water_D	.0000191	2.53e-06	7.54	0.000	.0000141 .0000241
ves_void	.0016072	.0000962	16.71	0.000	.0014179 .0017965

```
. regress Mn yield salinity ship_W water_D ves_void, noconstant
```

Source	SS	df	MS	Number of obs	=	300
Model	.012438881	5	.002487776	F(5, 295)	=	50581.78
Residual	.000014509	295	4.9183e-08	Prob > F	=	0.0000
				R-squared	=	0.9988

```
-----+-----
Total | .01245339      300 .000041511  Adj R-squared = 0.9988
Root MSE = .00022
```

```
-----+-----
Mn |      Coef.  Std. Err.      t    P>|t|    [95% Conf. Interval]
-----+-----
yield | -.0002411  4.34e-06   -55.50  0.000   -.0002496   -.0002325
salinity | -.000015  4.98e-06    -3.01  0.003   -.0000248   -5.21e-06
ship_W | .0001069  1.56e-06    68.42  0.000   .0001038   .0001099
water_D | .0001105  9.07e-06    12.19  0.000   .0000927   .0001283
ves_void | .0058541  .0003442    17.01  0.000   .0051767   .0065315
-----+-----
```

```
. regress Fe yield salinity ship_W water_D ves_void, noconstant
```

```
-----+-----
Source |      SS      df      MS      Number of obs =      300
-----+-----
Model | 60.5083362      5 12.1016672  F(5, 295) = 47352.93
Residual | .075391146     295 .000255563  Prob > F = 0.0000
-----+-----
Total | 60.5837273     300 .201945758  R-squared = 0.9988
Root MSE = 0.01597
Adj R-squared = 0.9987
```

```
-----+-----
Fe |      Coef.  Std. Err.      t    P>|t|    [95% Conf. Interval]
-----+-----
yield | -.0173048  .0003131   -55.27  0.000   -.017921   -.0166887
salinity | -.0008138  .0003589    -2.27  0.024   -.0015201   -.0001074
ship_W | .0077888  .0001126    69.19  0.000   .0075672   .0080103
water_D | .0059282  .0006536     9.07  0.000   .004642   .0072145
ves_void | .4282948  .0248112    17.26  0.000   .3794655   .4771241
-----+-----
```

```
. regress Ni yield salinity ship_W water_D ves_void, noconstant
```

```
-----+-----
Source |      SS      df      MS      Number of obs =      300
-----+-----
Model | .006315983      5 .001263197  F(5, 295) = 40328.09
Residual | 9.2403e-06     295 3.1323e-08  Prob > F = 0.0000
-----+-----
Total | .006325223     300 .000021084  R-squared = 0.9985
Root MSE = 0.00018
Adj R-squared = 0.9985
```

```
-----+-----
Ni |      Coef.  Std. Err.      t    P>|t|    [95% Conf. Interval]
-----+-----
yield | -.0002006  3.47e-06   -57.86  0.000   -.0002074   -.0001937
salinity | -8.49e-06  3.97e-06    -2.14  0.033   -.0000163   -6.73e-07
ship_W | .0000819  1.25e-06    65.73  0.000   .0000795   .0000844
water_D | .0000637  7.24e-06     8.81  0.000   .0000495   .000078
ves_void | .0045457  .0002747    16.55  0.000   .0040051   .0050863
-----+-----
```

```
. regress Cu yield salinity ship_W water_D ves_void, noconstant
```

```
-----+-----
Source |      SS      df      MS      Number of obs =      300
-----+-----
Model | .000329805      5 .000065961  F(5, 295) = 29664.07
Residual | 6.5596e-07     295 2.2236e-09  Prob > F = 0.0000
-----+-----
Total | .000330461     300 1.1015e-06  R-squared = 0.9980
Root MSE = 0.9980
Adj R-squared = 4.7e-05
```

```
-----+-----
Cu |      Coef.  Std. Err.      t    P>|t|    [95% Conf. Interval]
-----+-----
yield | -.00005  9.24e-07   -54.09  0.000   -.0000518   -.0000481
```

salinity		1.93e-06	1.06e-06	1.82	0.069	-1.52e-07	4.02e-06
ship_W		.0000237	3.32e-07	71.34	0.000	.000023	.0000243
water_D		-0.0000148	1.93e-06	-7.69	0.000	-0.0000186	-0.00011
ves_void		.0013364	.0000732	18.26	0.000	.0011924	.0014804

. regress Zn yield salinity ship\_W water\_D ves\_void, noconstant

Source		SS	df	MS	Number of obs	=	300
					F(5, 295)	=	18535.84
Model		2.5908e-08	5	5.1816e-09	Prob > F	=	0.0000
Residual		8.2466e-11	295	2.7955e-13	R-squared	=	0.9968
					Adj R-squared	=	0.9968
Total		2.5991e-08	300	8.6635e-11	Root MSE	=	5.3e-07

Zn		Coef.	Std. Err.	t	P> t	[95% Conf. Interval]
yield		5.83e-08	1.04e-08	5.63	0.000	3.79e-08 7.87e-08
salinity		-1.41e-07	1.19e-08	-11.91	0.000	-1.65e-07 -1.18e-07
ship_W		-3.25e-07	3.72e-09	-87.17	0.000	-3.32e-07 -3.17e-07
water_D		2.03e-06	2.16e-08	94.03	0.000	1.99e-06 2.08e-06
ves_void		-7.81e-06	8.21e-07	-9.51	0.000	-9.42e-06 -6.19e-06

. regress As yield salinity ship\_W water\_D ves\_void, noconstant

Source		SS	df	MS	Number of obs	=	300
					F(5, 295)	=	18535.84
Model		8.2480e-11	5	1.6496e-11	Prob > F	=	0.0000
Residual		2.6253e-13	295	8.8995e-16	R-squared	=	0.9968
					Adj R-squared	=	0.9968
Total		8.2742e-11	300	2.7581e-13	Root MSE	=	3.0e-08

As		Coef.	Std. Err.	t	P> t	[95% Conf. Interval]
yield		3.29e-09	5.84e-10	5.63	0.000	2.14e-09 4.44e-09
salinity		-7.98e-09	6.70e-10	-11.91	0.000	-9.30e-09 -6.66e-09
ship_W		-1.83e-08	2.10e-10	-87.17	0.000	-1.87e-08 -1.79e-08
water_D		1.15e-07	1.22e-09	94.03	0.000	1.12e-07 1.17e-07
ves_void		-4.40e-07	4.63e-08	-9.51	0.000	-5.32e-07 -3.49e-07

. regress Br yield salinity ship\_W water\_D ves\_void, noconstant

Source		SS	df	MS	Number of obs	=	300
					F(5, 295)	=	3145.61
Model		1.3840e-09	5	2.7680e-10	Prob > F	=	0.0000
Residual		2.5959e-11	295	8.7996e-14	R-squared	=	0.9816
					Adj R-squared	=	0.9813
Total		1.4100e-09	300	4.6999e-12	Root MSE	=	3.0e-07

Br		Coef.	Std. Err.	t	P> t	[95% Conf. Interval]
yield		1.19e-08	5.81e-09	2.05	0.041	4.96e-10 2.34e-08
salinity		6.11e-08	6.66e-09	9.17	0.000	4.80e-08 7.42e-08
ship_W		-6.34e-08	2.09e-09	-30.34	0.000	-6.75e-08 -5.93e-08
water_D		2.71e-07	1.21e-08	22.35	0.000	2.47e-07 2.95e-07
ves_void		-1.67e-06	4.60e-07	-3.63	0.000	-2.58e-06 -7.67e-07

. regress Sr yield salinity ship\_W water\_D ves\_void, noconstant

Source	SS	df	MS	Number of obs	=	300
Model	5.5360e-11	5	1.1072e-11	F(5, 295)	=	3145.61
Residual	1.0384e-12	295	3.5198e-15	Prob > F	=	0.0000
				R-squared	=	0.9816
				Adj R-squared	=	0.9813
Total	5.6399e-11	300	1.8800e-13	Root MSE	=	5.9e-08

Sr	Coef.	Std. Err.	t	P> t	[95% Conf. Interval]	
yield	2.39e-09	1.16e-09	2.05	0.041	9.92e-11	4.67e-09
salinity	1.22e-08	1.33e-09	9.17	0.000	9.59e-09	1.48e-08
ship_W	-1.27e-08	4.18e-10	-30.34	0.000	-1.35e-08	-1.19e-08
water_D	5.42e-08	2.43e-09	22.35	0.000	4.94e-08	5.90e-08
ves_void	-3.35e-07	9.21e-08	-3.63	0.000	-5.16e-07	-1.53e-07

. regress Mo yield salinity ship\_W water\_D ves\_void, noconstant

Source	SS	df	MS	Number of obs	=	300
Model	.000017416	5	3.4831e-06	F(5, 295)	=	29342.63
Residual	3.5018e-08	295	1.1871e-10	Prob > F	=	0.0000
				R-squared	=	0.9980
				Adj R-squared	=	0.9980
Total	.000017451	300	5.8169e-08	Root MSE	=	1.1e-05

Mo	Coef.	Std. Err.	t	P> t	[95% Conf. Interval]	
yield	-.0000115	2.13e-07	-54.06	0.000	-.000012	-.000011
salinity	4.64e-07	2.45e-07	1.90	0.059	-1.78e-08	9.45e-07
ship_W	5.51e-06	7.67e-08	71.79	0.000	5.36e-06	5.66e-06
water_D	-3.68e-06	4.45e-07	-8.26	0.000	-4.55e-06	-2.80e-06
ves_void	.0003094	.0000169	18.30	0.000	.0002761	.0003427

. regress Ag yield salinity ship\_W water\_D ves\_void, noconstant

Source	SS	df	MS	Number of obs	=	300
Model	3.0703e-12	5	6.1407e-13	F(5, 295)	=	18535.84
Residual	9.7730e-15	295	3.3129e-17	Prob > F	=	0.0000
				R-squared	=	0.9968
				Adj R-squared	=	0.9968
Total	3.0801e-12	300	1.0267e-14	Root MSE	=	5.8e-09

Ag	Coef.	Std. Err.	t	P> t	[95% Conf. Interval]	
yield	6.35e-10	1.13e-10	5.63	0.000	4.13e-10	8.57e-10
salinity	-1.54e-09	1.29e-10	-11.91	0.000	-1.79e-09	-1.28e-09
ship_W	-3.53e-09	4.05e-11	-87.17	0.000	-3.61e-09	-3.45e-09
water_D	2.21e-08	2.35e-10	94.03	0.000	2.17e-08	2.26e-08
ves_void	-8.50e-08	8.93e-09	-9.51	0.000	-1.03e-07	-6.74e-08

. regress Cd yield salinity ship\_W water\_D ves\_void, noconstant

Source	SS	df	MS	Number of obs	=	300
Model	1.5692e-12	5	3.1383e-13	F(5, 295)	=	18535.84
Residual	4.9947e-15	295	1.6931e-17	Prob > F	=	0.0000
				R-squared	=	0.9968
				Adj R-squared	=	0.9968
Total	1.5742e-12	300	5.2472e-15	Root MSE	=	4.1e-09



Cd	Coef.	Std. Err.	t	P> t	[95% Conf. Interval]	
yield	4.54e-10	8.06e-11	5.63	0.000	2.95e-10	6.12e-10
salinity	-1.10e-09	9.24e-11	-11.91	0.000	-1.28e-09	-9.19e-10
ship_W	-2.53e-09	2.90e-11	-87.17	0.000	-2.58e-09	-2.47e-09
water_D	1.58e-08	1.68e-10	94.03	0.000	1.55e-08	1.61e-08
ves_void	-6.08e-08	6.39e-09	-9.51	0.000	-7.33e-08	-4.82e-08

. regress Ba yield salinity ship\_W water\_D ves\_void, noconstant

Source	SS	df	MS	Number of obs	=	300
Model	.000038005	5	7.6009e-06	F(5, 295)	=	35983.02
Residual	6.2315e-08	295	2.1124e-10	Prob > F	=	0.0000
				R-squared	=	0.9984
				Adj R-squared	=	0.9983
Total	.000038067	300	1.2689e-07	Root MSE	=	1.5e-05

Ba	Coef.	Std. Err.	t	P> t	[95% Conf. Interval]	
yield	.000012	2.85e-07	42.10	0.000	.0000114	.0000125
salinity	-7.37e-06	3.26e-07	-22.59	0.000	-8.01e-06	-6.73e-06
ship_W	-5.29e-06	1.02e-07	-51.68	0.000	-5.49e-06	-5.09e-06
water_D	.0000555	5.94e-07	93.33	0.000	.0000543	.0000566
ves_void	-.0003523	.0000226	-15.62	0.000	-.0003967	-.0003079

. regress Pb yield salinity ship\_W water\_D ves\_void, noconstant

Source	SS	df	MS	Number of obs	=	300
Model	5.5608e-09	5	1.1122e-09	F(5, 295)	=	18535.84
Residual	1.7700e-11	295	6.0001e-14	Prob > F	=	0.0000
				R-squared	=	0.9968
				Adj R-squared	=	0.9968
Total	5.5785e-09	300	1.8595e-11	Root MSE	=	2.4e-07

Pb	Coef.	Std. Err.	t	P> t	[95% Conf. Interval]	
yield	2.70e-08	4.80e-09	5.63	0.000	1.76e-08	3.65e-08
salinity	-6.55e-08	5.50e-09	-11.91	0.000	-7.63e-08	-5.47e-08
ship_W	-1.50e-07	1.72e-09	-87.17	0.000	-1.54e-07	-1.47e-07
water_D	9.42e-07	1.00e-08	94.03	0.000	9.22e-07	9.61e-07
ves_void	-3.62e-06	3.80e-07	-9.51	0.000	-4.36e-06	-2.87e-06

## VITA

Captain Adam G. Seybert is currently serving as a US Army Nuclear Operations Officer. He holds an MS in Nuclear Engineering from the University of Tennessee and a BS in Mathematics from the United States Military Academy at West Point. He has served in many diverse positions throughout the military over the last ten years, including the Logistical Operations Officer for the 3<sup>rd</sup> Infantry Regiment (The Old Guard) and as a Medical Support Company Commander in the 101<sup>st</sup> Airborne Division (Air Assault). He has deployed to both Iraq and Afghanistan and has experience with planning consequence management operations in urban environments.